nano newsletter

nº 11

NanoSpain - Special Issue

March 2008

http://www.phantomsnet.net

NanoSpain.org

Red Española de Nanotecnología

Spanish Nanotechnology Network

CIC nanoGUNE

nanoscience cooperative research center

The Nanoscience Cooperative Research Center CIC nanoGUNE Consolider invites applications and nominations for two positions as

Group Leaders

CIC nanoGUNE Consolider, located in San Sebastián, Basque Country (Spain), is a research center created recently with the mission of conducting basic and applied world-class research in nanoscience and nanotechnology, fostering training and education excellence, and supporting the growth of a nanotechnology-based industry.

The Group Leaders of nanoGUNE will be responsible for the design, management, and operation of their respective Research Area and laboratories. At the present time, nanoGUNE is welcoming applicants in the following disciplines:

• **Nanoscale Devices** (#001). All qualified candidates will be considered. Special preference might be given to candidates specializing in nanomechanical, nanofluidic, nanobiological, nanomagnetic or optoelectronic devices or technologies.

• **Nanoscale Imaging** (#002). All qualified candidates will be considered. Special preference might be given to candidates specializing in electron microscopy or scanning probe microscopy techniques.

Candidates should have an outstanding track record of research, with an orientation to nanoscience and nanotechnology, a proven ability to obtain competitive research funding, and a proven record of technological transfer initiatives. Proficiency in spoken and written English is compulsory; knowledge of Spanish is not a requirement. An attractive remuneration will be offered.

Applicants should forward their CV, a summary of research interests, and a list of at least three references to director@nanogune.eu **before 15 April 2008.**

E nano newsletter

Editorial Information

Research / Nanospain

CMOS-integrated nanomechanical resonators as versatile and ultra-sensitive mass sensors 5

J. Arcamone, M. A. F van den Boogaart, T. Ondarçuhu, E. Dujardin, F. Serra-Graells, G. Abadal, N. Barniol, J. Brugger and F. Pérez-Murano

Glyconanoparticles for biomedical applications: Dynamic AFM and opto-magnetic detection of molecular interactions 10

M. Luna, M. Köber, M. Fuss, F. Briones, G. Ochoa, J. M. de la Fuente and S. Penades

Magneto-plasmonic materials: tuning magneto-optics with plasmons 15

G. Armelles, A. Cebollada, A. García-Martín, J.M. García-Martín, J.V. Anguita, J.B. González-Díaz, J.F. Torrado and E. Ferreiro

NANO Vacancies 20

NANO Conferences 22

NANO News 24

Research / Nanospain

Design and production of micro and nanostructured polymer substrates for cell culture applications 25

E. Martínez, C.A. Mills, A. Lagunas, M. Estévez, S. Rodríguez-Segui, J. Comelles, S. Oberhansl and J. Samitier

An easy to scale-up preparation of unirrom unilamellar nanovesicles using CO_2 - expanded solvents 28

M. Cano, S.Sala, N. Ventosa and J. Veciana

Optical resonances in finite arrays of dielectric nanorods 31

S. Albaladejo, M. Laroche and J.J. Sáenz

Dear Readers:

This E-Nano newsletter issue contains several articles of the coordinators of the Spanish Nanotechnology Network (NanoSpain) Working Groups covering the following areas: Nanofabrication; Nanobiotechnology/ Nanomedicine; Nanochemistry, Nanophotonics and Theory & Modelling, currently very active in Spain.

Depósito Legal: M-43078-2005

The NanoSpain network involves 241 groups belonging to research institutes and industry with around 2000 researchers, being one of the biggest networks in Spain. The mission of its Working Groups consists in enhancing the communication among the Spanish research community, investigating opportunities that promote collaborations among NanoSpain members, looking for areas of common ground between different technologies, etc.

Expected impact of initiatives such as this NanoSpain contribution to the E-Nano Newsletter is to enhance visibility, communication and networking between members, facilitate rapid information flow and therefore shape and consolidate the Spanish research community.

We would like to thank all the authors who contributed to this issue as well as the "Ministerio de Educación y Ciencia" (MEC) for the financial support (project NAN2006-26554 E y D).

Dr. Antonio Correia

E nano newsletter Editor

Phantoms Foundation

EDITORIAL INFORMATION

E nano newsletter **nº11** March 2008

Published by **Phantoms Foundation** (Spain)

Editor: Dr. Antonio Correia (Phantoms Foundation)
antonio@phantomsnet.net

Assistant Editor: Jose Luis Roldan (Phantoms Foundation)
jlroldan@phantomsnet.net

1500 copies of this issue have been printed

Full color newsletter available at:
http://www.phantomsnet.net/Foundation/newsletters.php

For any question please contact the editor at:
antonio@phantomsnet.net

Editorial Board: Adriana Gil (Nanotec SL, Spain), Christian Joachim (CEMES-CNRS, France), Ron Reifenberger (Purdue University, USA), Stephan Roche (CEA-INAC, France), Juan Jose Saenz (UAM, Spain), Pedro A. Serena (ICMM-CSIC, Spain), Didier Tonneau (CRMC2-CNRS, France), Rainer Waser (Research Center Julich, Germany)

CHALMERS

MC2 ACCESS

To research groups in
EU, associate and candidate countries:

We offer free access to advanced processing for microwave electronics, photonics and nanotechnology.

Through an EU-financed programme we offer free access to advanced micro- and nanotechnology device processing environments for microwave and photonic devices, MEMS structures and for nanotechnology at the Department of Microtechnology and Nanoscience (MC2), Chalmers University of Technology, in Göteborg, Sweden. This offer is open for visiting researchers as well as remote users, both from universities and SMEs (small and medium size enterprises).

The facility provides means to develop process steps, process sequences, and components in small/medium quantities. In 1240 m² of clean-room area, more than 170 tools are available, including two e-beam lithography systems, silicon processing on up to 150 mm wafers, III-V and wide bandgap processing, molecular beam epitaxy, CVD and dry etching systems.

Only research groups that are entitled to disseminate the knowledge they have generated under the project are eligible to benefit from access to the infrastructure under the contract. **NOTE!** The sole exception to this rule are user groups from an SME that wish to use the infrastructure for the first time.

Contract No: 026029
Contract Period: 2006-2009

Project Manager:
Associate Professor
Ulf Södervall
access@mc2.chalmers.se

MC2
Microtechnology and Nanoscience

www.mc2.chalmers.se/MC2ACCESS

CMOS-integrated nanomechanical resonators as versatile and ultra-sensitive mass sensors

J. Arcamone[1,4,#], M. A. F. van den Boogaart[2], T. Ondarçuhu[3], E. Dujardin[3], F. Serra-Graells[1], G. Abadal[1], N. Barniol[1], J. Brugger[2] and F. Pérez-Murano[1,]*

[1]CNM-IMB (CSIC) and ECAS-UAB, Campus UAB, E-08193 Bellaterra (Barcelona), Spain
[2]Microsystems Laboratory (LMIS1), EPFL, CH-1015 Lausanne, Switzerland
[3]CEMES-CNRS, 29 rue Jeanne Marvig, 31055 Toulouse cedex 4, France
[4]Now at CEA/LETI/MINATEC, DIHS-LCMS, 17 rue des Martyrs, 38054 Grenoble Cedex 9 (France)
[#]julien.arcamone@cea.fr; [*]Francesc.Perez@cnm.es

Introduction

Mechanical resonators with submicron dimensions are a specific type of nano-electromechanical systems (NEMS). They feature outstanding properties as physical or (bio)chemical sensors **[1]**, or as building blocks for high-frequency telecommunication systems **[2]**. Their practical applications would benefit much from on-chip signal processing, whereby optimal performance is achieved in case of monolithic integration with CMOS. Such NEMS/CMOS made of silicon are indeed very promising systems combining unique sensing attributes, thanks to the high resonance frequency mobile mechanical part, with the possibility to electrically detect the output signal in enhanced conditions and for portable applications.

In terms of technology, combining fabrication of silicon nanomechanical resonators with a CMOS technology is challenging. In this work, we used a new wafer-scale technological process based on post-processing CMOS circuits using nanostencil lithography (nSL) **[3,4]**. As it will be shown, we have succeeded in the parallel definition and fabrication of thousands of Si nanomechanical resonators at the 200nm scale monolithically integrated with a CMOS circuit. Their functionality is demonstrated by electrically measuring their resonance spectra.

In the last section, we give two examples of applications of Si NEMS/CMOS that illustrate their high performance as versatile and ultra-sensitive mass sensors. They exhibit the potential to replace quartz-crystal microbalances. First, cantilever type-nanoresonators placed in a high-vacuum evaporation chamber are used to monitor in-situ the deposition of sub-nm thick gold layers **[3]**. Second, a specific design of nanoresonators is used to study the evaporation in air of minuscule sessile liquid droplets deposited by nanodispensing techniques **[5]**.

Keywords: NEMS, Nanomechanical resonant sensors, nanofabrication, nanostencil lithography CMOS integration

I. Integration of NEMS on CMOS

1. A CMOS circuit for interfacing electrostatic silicon NEMS resonators

Electrostatic actuation and capacitive readout by an integrated circuit (IC) are used for detecting the oscillations of Si nanomechanical resonators in the MHz range. A monolithic integration drastically improves the electrical readout since parasitic capacitances are strongly reduced at the resonator output. Furthermore, it allows 'on-chip' signal processing (amplification and conditioning). Thus, when electrostatically driving the resonator by a DC+AC voltage, the readout electrode, electrically connected to the IC input, collects a capacitive current, one part of this current being specifically generated by the variation of electrode-resonator capacitance due to the mechanical motion itself. A new interfacing CMOS circuit **[6]**, based on a second generation current conveyor (CCII), was designed to read out this current. This circuit ensures a constant voltage biasing at the resonator output, while it amplifies the readout current and converts it to an output voltage according to an external load resistor. Special areas, interconnected to the circuits input, are reserved for the integration of nanodevices (**see Figure 1**).

2. Post-processing of CMOS wafers by nanostencil lithography

We use a post-processing approach in which CMOS circuits are first fabricated according to a standard CMOS technology, then NEMS are subsequently patterned and fully fabricated **[7]**.

For defining NEMS on CMOS, nanostencil lithography (nSL) **[4]** ensures a parallel patterning for rapid processing at wafer scale, and a definition of features in the 100nm range. This is a flexible, simple, yet powerful, parallel and resistless patterning method based on a high-resolution wafer-scaled shadow mask. In the present work, full-wafer (100mm diameter) nanostencil fabrication is based on advanced bulk and surface micromachining **[8]**: the stencil frame is a micromachined Si wafer containing hundreds of nanostencils under the form of 200nm

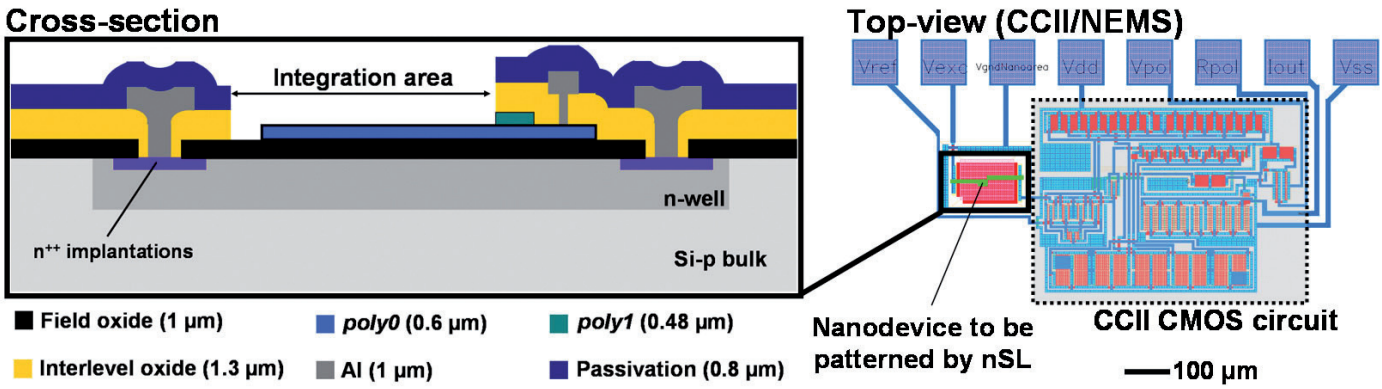

Figure 1. *CMOS circuit layout. Inset: detail of an integration area for nanoresonator post-fabrication.*

thick free-standing silicon nitride (SiN) membranes with micro- and nano-scale apertures.

In this approach, existing CMOS layers used as structural layer (600nm thick polySi) and sacrificial layer (1µm thick field SiO_2) of the resonators. The first post-processing step consists in a full-wafer, single step, patterning of all integration areas by evaporation of an 80nm thick Al layer using nSL (**figure 2a**). For this purpose, CMOS and nanostencil wafers are optically aligned with a dedicated tool. By this method, an alignment accuracy of 1µm is achieved at wafer scale. The resulting Al patterns are then corrected by a partial dry etching that eliminates the pattern blurring caused by the presence of a gap between the stencil and the surface of the integration area due to the CMOS wafer topography **[9]**. After recovering their nominal dimensions, these patterns are transferred to the 600nm thick polysilicon structural layer by reactive ion etching using them as a mask (**figure 2b**). Al is chosen as deposition material because of its very high dry etching selectivity with respect to silicon. The last step (**figure 2c**) consists in releasing the resonators and removing the Al mask by a local wet etching based on HF acid. The circuit is robustly protected during this etching by an adequately annealed photoresist layer, in which apertures are defined only around the resonators.

Applying this full-wafer technology, we have finally obtained CMOS wafers containing each ~2000 fully fabricated nanomechanical devices of diverse types, and which are connected to CMOS circuits for signal interfacing and amplification. Mechanical structures with line widths down to 200nm can be routinely achieved by means of the presented process sequence **[3]**.

3. Electrical characterization of NEMS/CMOS resonators

Figure 3 shows resonance spectra (a) in air and (b) in vacuum (at 10^{-2} mBar) of an in-plane vibrating cantilever fabricated according to this technology. Such nanocantilevers typically have the following dimensions: length = 14.5µm, width = 250nm and thickness = 600nm. These spectra have been electrically measured through the CCII CMOS circuitry with a network analyzer. The obtained quality factors are about 10 and 8000 in air and vacuum respectively. The resonance frequency can be tuned by varying the applied DC voltage ($V_{IN\ DC}$). Interestingly, low driving voltages are enough for polarizing the devices: $V_{IN\ DC}$ is around 1V in vacuum and around 10V in air, added to a 0.2V AC.

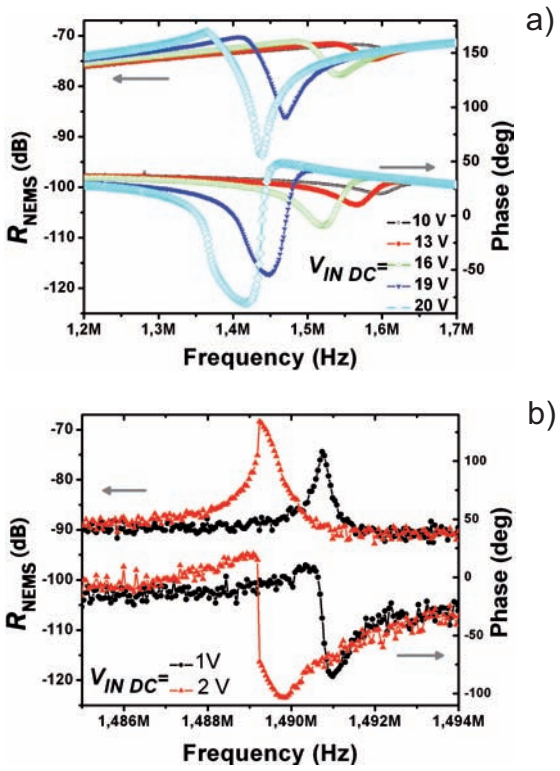

Figure 3. *Resonance spectra in (a) air and (b) vacuum of CMOS integrated in-plane vibrating cantilevers.*

II. NEMS/CMOS as high performance mass sensors

Compared to widely used quartz-crystal microbalances (QCM), Si-based nanomechanical resonators applied as mass sensors offer clear advantages in terms of sensitivity and system integration. For scientific purposes, they constitute new tools for the study of previously unexplored chemical, physical or biological mechanisms. Regarding industrial applications, they could potentially replace QCM in a near future for the monitoring of thin layers deposition

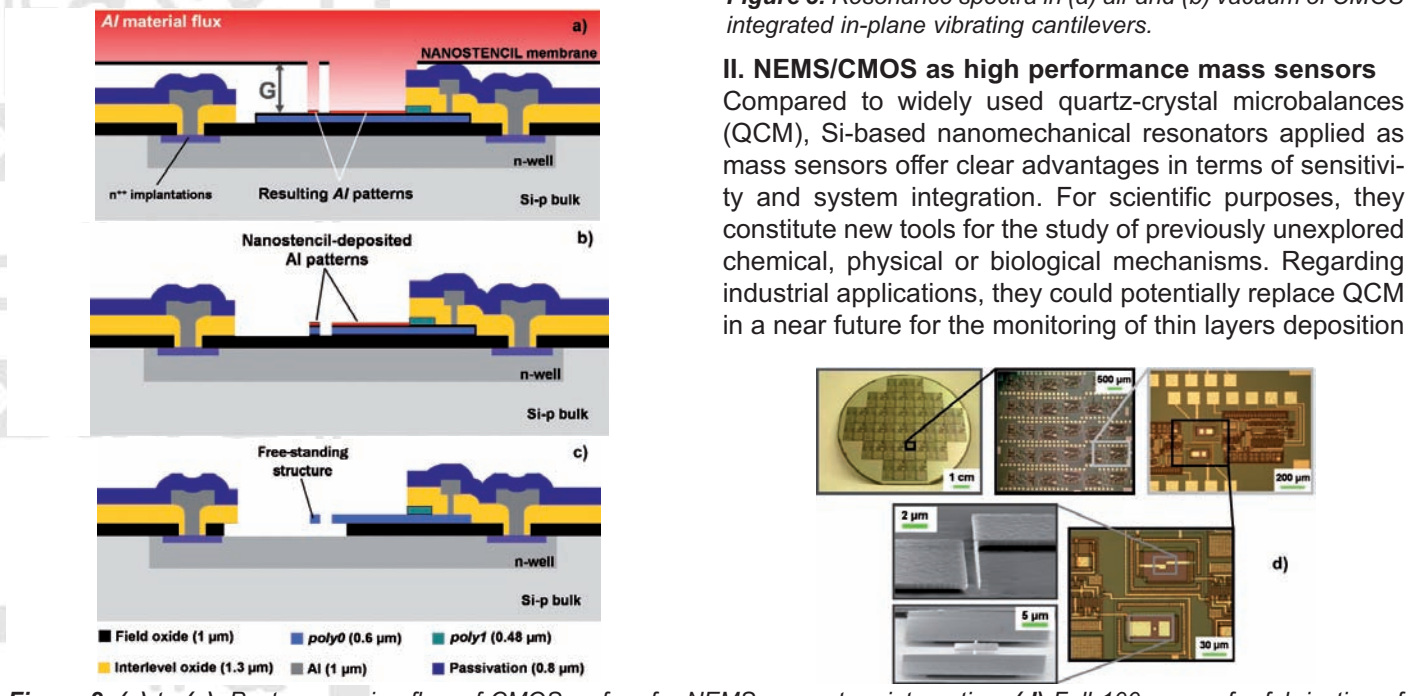

Figure 2. ***(a)*** *to* ***(c).*** *Post-processing flow of CMOS wafers for NEMS resonators integration.* ***(d)*** *Full 100-mm-wafer fabrication of diverse types of nanoresonators, patterned at full-wafer scale in one single step by nSL and monolithically connected to the CCII CMOS circuit for signal interfacing.*

in semiconductor processing systems. The principle of operation of the sensor is based on the detection of the negative shift of resonance frequency when a small quantity of mass is deposited on top of the mechanical structure. Through two experiments, we demonstrate the functionality and the performance of NEMS/CMOS mass sensors.

1. Monitoring the deposition of ultra-thin layers

We have monitored the deposition of ultra-thin gold layers by measuring in situ and in real-time the evolution of the phase signal of a NEMS/CMOS cantilever (see figure 2d) placed in an evaporation chamber. The deposited average gold thickness is so thin (inferior to a monolayer) that we entirely attribute the globally negative resonance frequency shift to mass loading and neglecting adsorption-induced stiffening effects.

Four sequential 40 seconds long depositions of gold have been performed while driving the cantilever at a constant frequency of 2.92MHz (close to its resonance frequency). The change of phase signal is monitored. The detail of the phase signal evolution is shown in **figure 4a**: grey bars indicate when the evaporation shutter is open, i.e. when gold is deposited on the cantilever. By means of a mathematical treatment, it is possible to convert the phase signal into a real-time evolution of the resonance frequency: **figure 4b** depicts the resulting curve (left vertical axis). The mass deposition curve coherently features (i) flat plateaus when the shutter is closed and (ii) linear shifts upwards during the depositions. The total deposited thickness is globally inferior to 0.1nm, what indicates that not

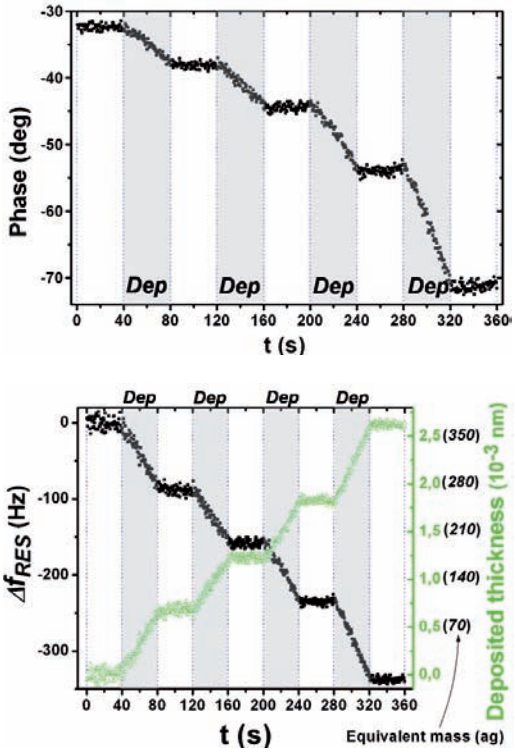

Figure 4. (a) *Phase monitoring at a constant frequency (~2.92 MHz), in a 6 minutes time span during which 4 depositions (see grey bars) of 40s each are performed.* ***(b)*** *Corresponding evolution of resonance frequency shift obtained by the transformation of the phase curve. The green curve is the corresponding time evolution of the deposited thickness. In brackets, the deposited mass corresponding to a given thickness is indicated.*

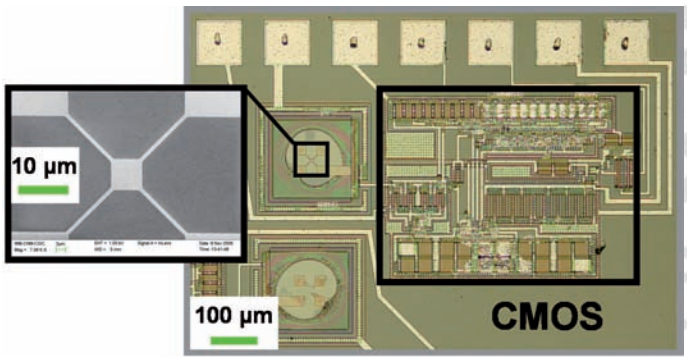

Figure 5. *Images of a QBR monolithically integrated with a CCII CMOS circuit. The device has the following dimensions: central plate (6*6µm²), beams width and length: 600nm and 13.5µm, thickness: 500nm.*

even a monolayer is formed on the cantilever surface. A simultaneously operated QCM has systematically exhibited resonance frequency shifts about three orders of magnitude smaller than CMOS nanocantilevers what demonstrates the high performance as areal mass sensors of such NEMS/CMOS.

2. Monitoring the evaporation in air of femtoliter sessile droplets

We present a time-resolved study of the evaporation in air of minuscule sessile droplets deposited by a nanodispensing technique called NADIS **[10]**. Nanomechanical resonators are used to determine with high precision the mass loss of liquid droplets with time. Indeed, in recent years the need of methods to manipulate very small liquid quantities has emerged, leading to the development of nanofluidics or nanodispensing techniques. At these scales, evaporation processes become important. However, previous comprehensive studies of evaporation are limited to microliter droplets **[11]**. We have addressed the question of the validity of the macroscopic models at the micron scale **[5]**, which corresponds to volumes of femtoliters, nine orders of magnitude smaller than previously published data.

The resonator is a CMOS-integrated polysilicon micro quad-beam with arms in the nanometer length (**see figure 5**). A QBR operated in its vertical flexion fundamental mode (in the MHz range) provides high mass sensitivity together with large active area for convenient droplet deposition. When depositing mass on its central plate, the resonator remains relatively insensitive both to the adsorbate stiffness (which ensures the mass loading effect is mechanically dominant) and position.

Prior to the evaporation experiments, QBR were calibrated by successive loading of silica beads (with well-defined mass: 4.5pg each) using a micro-manipulator. The obtained mass resolution is three orders of magnitude better than commercial QCM. Nanodispensing of droplets was based on the use of modified AFM cantilevers, as described in **[10]**. The liquid is transferred from a reservoir droplet on the cantilever to the surface through a nanochannel drilled at the tip apex by focused ion beam (FIB). Although ultimate droplets dimensions of 75nm were demonstrated, tips used in this study had an aperture of 300nm in diameter and hydrophilic outer walls in order to deposit micron-sized droplets. For deposition

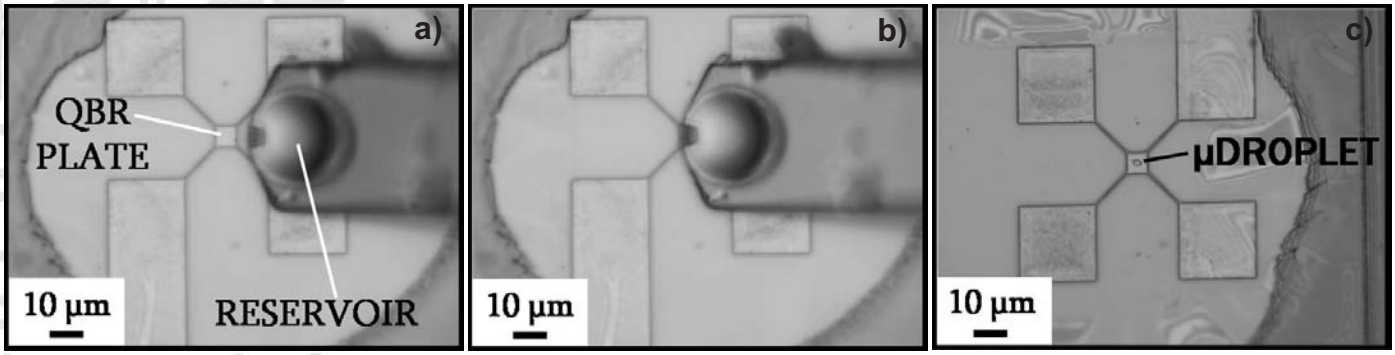

Figure 6. *Optical images of the deposition procedure.* ***(a)*** *the pre-loaded NADIS tip is approached from the surface;* ***(b)*** *the QBR is positioned under the tip with the nanopositioning table;* ***(c)*** *after contact, the tip is withdrawn leaving a droplet on the surface.*

(**see figure 6**), the tip was approached a few microns from the surface. Alignment with the resonator was then performed using a nanopositioning table incorporated in the sample holder of our AFM set-up **[12]**. Droplets with diameters ranging from 1 to 5µm were reproducibly deposited on the resonators by adjusting the contact time. This method was soft enough to keep the resonator properties intact.

During evaporation of glycerol droplets, we monitored the resonance frequency shift of the QBR (**figure 7a**). Using the calibration curve, the temporal evolution of the droplets mass is determined down to 10fg (10 attoliter in volume) resolution. Examples of results obtained on droplets with initial volumes ranging from 0.2fL to 20fL are shown on **figure 7b**. The mass decreases nonlinearly, with a slowing down of the evaporation rate along the process. Optical observations during evaporation showed that the droplets diameter decreases with time. This is characteristic of an evaporation mode on hydrophobic surfaces with a constant contact angle between droplet and surface. A detailed analysis of the results showed that the laws governing evaporation at the macroscopic scale are still valid for microdroplets of femtoliter volumes **[5]**.

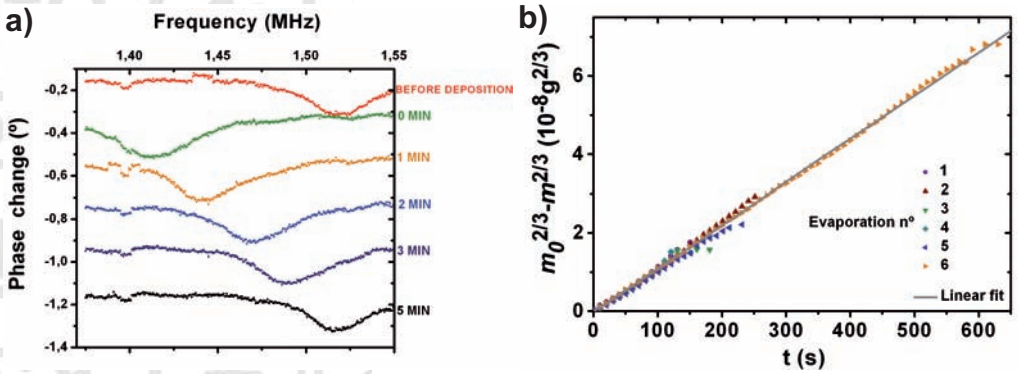

Figure 7. ***(a)*** *Resonance frequency shifts along the evaporation process.* ***(b)*** *Temporal evolution of the mass of droplets of different sizes (initial volumes ranging from 0.2 to 20 fL).*

Conclusion

This letter presents the technology for the full wafer integration of NEMS on CMOS. In this frame, the potential of nanostencil lithography as a parallel, straightforward patterning technique to define devices on CMOS at the 200nm scale has been demonstrated. A series of standard 100mm CMOS wafers were post-processed according to this technique: this resulted in the complete fabrication of about 2000 resonators per wafer, monolithically interconnected with a CMOS readout circuit. The work reported here represents the first time, to our knowledge, that an emerging nanolithography technique has been used to pattern multiple N-MEMS devices on a whole CMOS wafer in a parallel and relatively low-cost approach. In terms of device functionality, the mechanical resonance of fully integrated nanomechanical resonators has been successfully sensed by the CMOS circuit according to a capacitive detection scheme.

The potential of NEMS/CMOS resonators as ultra-sensitive mass sensors has been further illustrated through two experiments. The successful monitoring using these devices of (i) the deposition of ultra-thin gold layers in vacuum and (ii) the evaporation in air of femtoliter sessile droplets clearly demonstrates their much better performances than QCM in terms of sensitivity and resolution.

Acknowledgments

The authors are very grateful to Dr. Jordi Fraxedas for the gold deposition experiments. This project is partially funded by the European Commission within the project NaPa and the Swiss Federal Office for Education and Science (OFES), and by Swiss National Science Foundation, project NANO-IC.

References

[1] M. Li, H. X. Tang, and M. L. Roukes, *"Ultra-sensitive NEMS-based cantilevers for sensing, scanned probe and very high-frequency applications,"* **Nature Nanotechnology, vol. 2, pp. 114-120, 2007**.

[2] C. T. C. Nguyen, *"MEMS technology for timing and frequency control,"* **IEEE Transactions on Ultrasonics Ferroelectrics and Frequency Control, vol. 54, pp. 251-270, 2007**.

[3] J. Arcamone, M. A. F. van den Boogaart, F. Serra-Graells, J. Fraxedas, J. Brugger, and F. Perez-Murano, *"Full-wafer fabrication by nanostencil lithography of nano/micromechanical mass sensors monolithically integrated with CMOS,"* **Nanotechnology, vol. to be published, 2008.**

[4] J. Brugger et al., *"Quick & Clean: Advances in high resolution Stencil Lithography,"* **E-Nano Newsletter, vol. 8, pp. 22-28, June 2007.**

[5] J. Arcamone, E. Dujardin, G. Rius, F. Pérez-Murano, and T. Ondarcuhu, *"Evaporation of Femtoliter Sessile Droplets Monitored with Nanomechanical Mass Sensors,"* **Journal of Physical Chemistry B, vol. 111, pp. 13020-13027, 2007.**

[6] J. Arcamone, B. Misischi, F. Serra-Graells, M. A. F. van den

imdea nanociencia

Molecular Nanoscience
Array of PCBM molecules on Au(111)

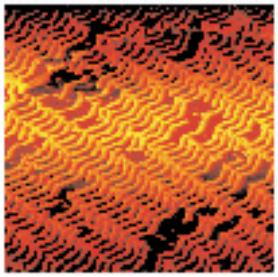

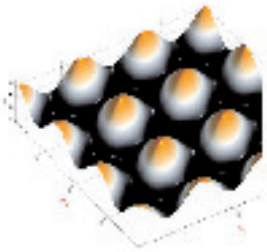

Nanoscience at very low temperatures
Potential landscape of a superconducting qubits

Nanoelectronics Nanophotonics
Photonic crystals

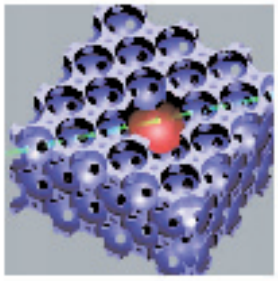

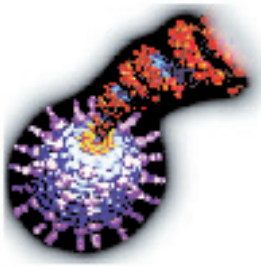

Biomachines and manipulation of biomolecules
Biological molecular motors

Nanomagnetism and the biomedical application of magnetic nanoparticles
Magnetic nanoparticles inside tumoral cells

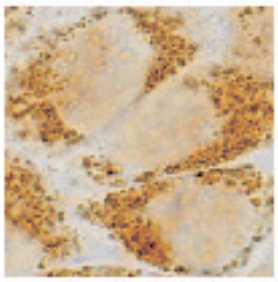

Nanofabrication and advanced instrumentation
Molecular smile assembled with STM

IMDEA- Nanociencia is a private Foundation created by joint initiative of the regional Government of Madrid and the Ministry of Education of the Government of Spain in February 2007 to manage a new research institute in Nanoscience and Nanotechnology (IMDEA-Nanociencia), which is located in the campus of the Universidad Autónoma de Madrid, 12 km away from Madrid downtown with an excellent communication by public transportation with the Madrid-Barajas airport (25-30 min) and Madrid downtown (15-20 min).

The institute offers attractive opportunities to develop a career in science at various levels from Ph.D. students to senior staff positions.

INTERNATIONAL CALL FOR RESEARCH POSITIONS 2008 REOPENED.
The deadline for applications is April 19, 2008. For more information see http://www.imdea.org/Default.aspx?tabid=985

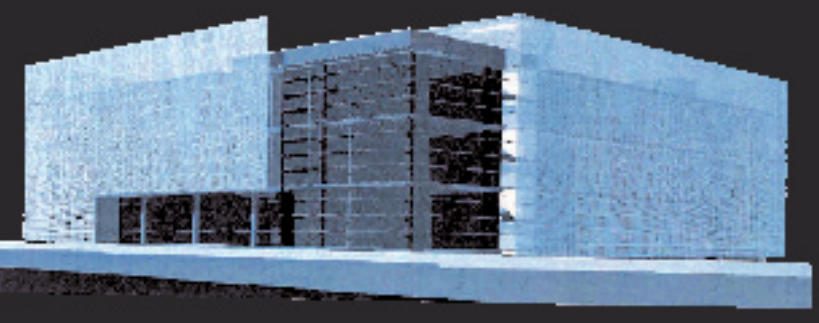

Contact
IMDEA Institute of Advanced Studies in Nanoscience (IMDEA-Nanociencia)
Facultad de Ciencias, C-IX, 3rd floor
Campus de Cantoblanco Madrid 28049 Spain

Phone 34 91 497 06 49 / 06 51 / 06 54 Fax 34 91 497 06 55
contact@imdea.org
For further details see http://www.imdea.org

Boogaart, J. Brugger, F. Torres, G. Abadal, N. Barniol, and F. Perez-Murano, *"A Compact and Low-Power CMOS Circuit for Fully Integrated NEMS Resonators,"* **IEEE Transactions on Circuits and Systems II, vol. 54, pp. 377-381, 2007.**

[7] J. Verd, G. Abadal, M. Villarroya, J. Teva, A. Uranga, F. Campabadal, J. Esteve, E .Figueras, F. Pérez-Murano, Z. Davis, E. Forsen, A. Boisen, N. Barniol. *"Design, Fabrication, and Characterization of a Submicro-electromechanical Resonator with Monolithically Integrated CMOS Readout Circuit"* **Journal of Micro-electromechanical Systems, 14, 508-519 (2005)**

[8] M. A. F. van den Boogaart, G. M. Kim, R. Pellens, J. P. van den Heuvel, and J. Brugger, *"Deep-ultraviolet-microelectromechanical systems stencils for high-throughput resistless. patterning of mesoscopic structures,"* **Journal of Vacuum Science & Technology B, vol. 22, pp. 3174-3177, 2004.**

[9] J. Arcamone, A. Sanchez-Amores, J. Montserrat, M. A. F. van den Boogaart, J. Brugger, and F. Perez-Murano, *"Dry etching for the correction of gap-induced blurring and improved pattern resolution in nanostencil lithography,"* **Journal of Micro/Nanolithography, MEMS and MOEMS, vol. 6, pp. 013005-7, 2007.**

[10] A. P. Fang, E. Dujardin, and T. Ondarcuhu, *"Control of droplet size in liquid nanodispensing,"* **Nano Letters, vol. 6, pp. 2368-2374, 2006.**

[11] R. G. Picknett and R. Bexon, *"Evaporation of Sessile or Pendant Drops in Still Air,"* **Journal of Colloid and Interface Science, vol. 61, pp. 336-350, 1977.**

[12] T. Ondarcuhu, L. Nicu, S. Cholet, C. Bergaud, S. Gerdes, and C. Joachim, *"A metallic microcantilever electric contact probe array incorporated in an atomic force microscope,"* **Review of Scientific Instruments, vol. 71, pp. 2087-2093, 2000.**

Glyconanoparticles for biomedical applications: Dynamic AFM and opto-magnetic detection of molecular interactions

Mónica Luna, Mariana Köber, Martina Fuss, Fernando Briones*

IMM-CSIC, E-28760 Tres Cantos, Spain

Isabel García, Jesus M. de la Fuente† and Soledad Penades, CIC-BiomaGUNE, CIBER-BBN, Parque Tecnológico, E-50009 Zaragoza, Spain

Gorka Ochoa, PROGENIKA Biopharma S.A., E-20009 San Sebastián, Spain
email: **mluna@imm.cnm.csic.es*
† Present address: INA, University of Zaragoza, E-50009 Zaragoza, Spain

biofunctional magnetic nanoparticles and biomolecules by dynamic SPM, force spectroscopy and novel opto-magnetic methods.

Keywords: Nanoparticles, molecular recognition, biomedical applications, dynamic AFM, opto-magnetic methods

Introduction

The excellent properties of magnetic glyconanoparticles regarding their stability, solubilitiy in water, their small size **[1]** and magnetic properties **[2]** make them ideal candidates for important biomedical applications. By a convenient biological functionalization of these nanoparticles they can be directed for drug delivery **[3]**, follow the growth and the trajectory of cells **[4]** or can be used as contrast agents in nuclear magnetic resonance imaging **[5]**. The success of the biomedical applications related to biofunctional magnetic nanoparticles relies on the ability of these nanoparticles to recognize their final target. Thus, our work is devoted to the study of interactions between biofunctional magnetic nanoparticles and biomolecules by dynamic SPM, force spectroscopy and novel opto-magnetic methods.

Ultra small gold glyconanoparticles as DNA-condensing agents: a Non-contact and Electrostatic Force Microscopy analysis

DNA condensation, the process by which DNA molecules are compacted into a globular shape, is an important biological event involved, for example, in the organization of DNA into chromatin **[6,7]**. Recently, there has been an increasing interest toward this phenomenon because it represents a fundamental step in non-viral gene delivery **[8].** So far, most efforts concentrated on using cationic lipids or polymers as condensing agents **[9]**. However, in more recent times, the interaction of DNA with inorganic nanoparticles of defined size and shape has attracted much attention due to their high potential **[10]**.

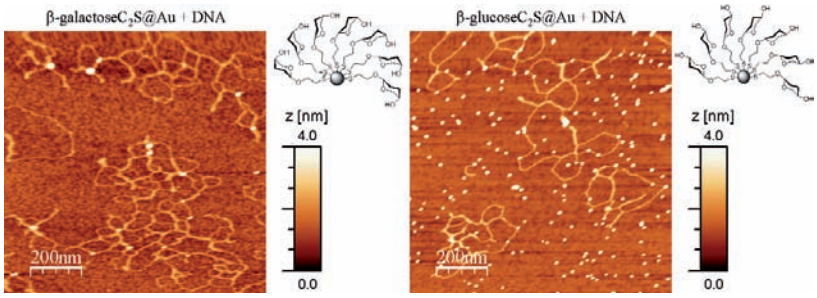

Figure 1. *Nanoparticles covered only by a shell of β-galactose monosaccharides (left) and β-glucose monosaccharides (right) incubated with DNA. The plasmid is unwrapped.*

Encouraged by first results evidencing the condensation capacity of amine groups present in the organic coverage of the metallic glyconanoparticles **[11]** our research activities are concerned with further analysis of the condensation ability of hybrid gold glyconanoparticles functionalized with various carbohydrates and amine-ending linkers by means of non-contact force microscopy and electrostatic force microscopy **[12].** For this purpose DNA is incubated with gold GNPs (1.5-2nm of diameter) that vary in their organic coverage. The organic coverage is either composed of only monosaccharides or of a 1:1 mixture of monosaccharides and amine-ending linkers. The monosaccharides employed were α-galactose, β-galactose and β-glucose. The DNA used in our experiments is the circular plasmid pEGFP-N1.

Two important results have been obtained. First, particles covered by different monosaccharides (but no amine-ending linkers) show differences in the interaction with the DNA. As can be seen in **Figure 1 (left)** particles functionalized with β-galactose are mainly situated on top of the plasmid whereas the particles functionalized with β-glucose and α-galactose are found equally on top of the DNA and aside (**Figure 1, right**). The second important observation is that the plasmid presents an open conformation when no amine ending groups are present (Figure 1) whereas when the coverage of the particles is formed by a 1:1 mixture of β-glucose and an amine-ending polyethylene glycol (PEG) linker the strong electrostatic interaction

between the positively charged amines and the negatively charged DNA phosphate groups induces the wrapping of the DNA molecules around the nanoparticles, as can be observed in **Figure 2**. The size of the condensed globes is less than 100 nm which is an important fact since in experiments documented in literature structures of this size were able to cross the cell membrane and transfect.

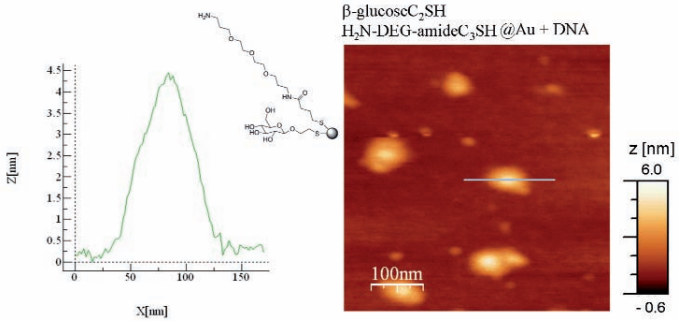

Figure 2. *Nanoparticles covered by a 1:1 mixture of β-glucose and an amine-ending polyethylene glycol (PEG) linker incubated with DNA. Strong electrostatic interactions between the amines and the DNA phosphate groups lead to the wrapping of the DNA molecules around the GNPs. The size of the globes is less than 100 nm.*

Supramolecular self-assembled arrangements of maltose glyconanoparticles

In one experiment, the magnetic Au-Fe_xO_y nanoparticles were capped with the neoglycolipid 11,11'-dithiobis[undecanyl-β-maltoside] **1 (Figure 3).** After the nanoparticles were isolated from the methanolic solution by decantation we could obtain, after evaporation, a white residue which was also soluble in water. During the examination of this fraction by TEM, once dried on an amorphous carbon support, we observed **[13]** nanoparticles well ordered in a kind of polymeric parallel arrangement. The decanted fraction provides TEM images with randomly distributed nanoparticles. Thus, as can be seen in Figure 3, two different types of structures were isolated: one where the nanoparticles are aligned, ***malto*-Au-Fe_xO_y (polymer)**, and another with non-ordered nanoparticles, ***malto*-Au-Fe_xO_y**.

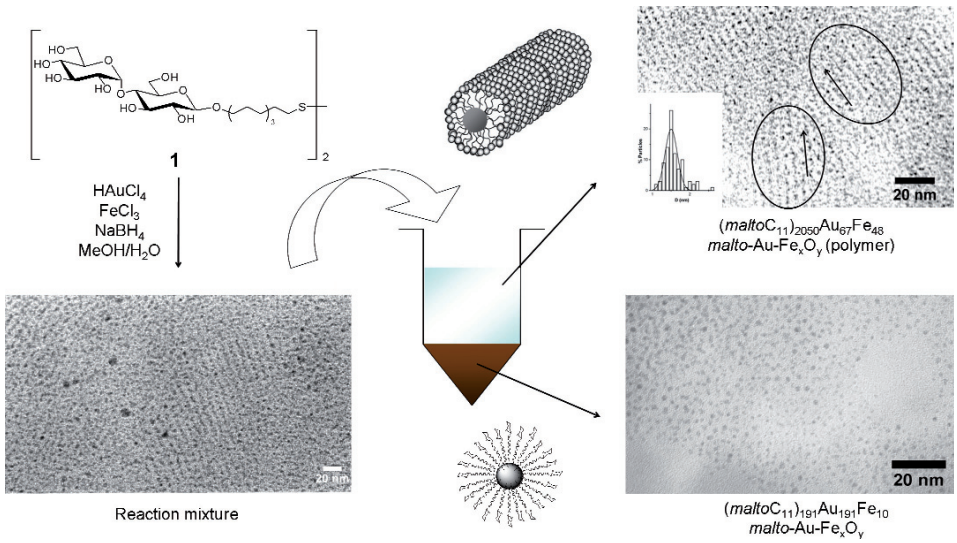

Figure 3. *Cartoon illustrating the synthesis and isolation of **malto-Au-Fe_xO_y** and **malto-Au-Fe_xO_y (polymer)** nanostructures. Transmission electron micrographs of the reaction crude and the two fractions separated are shown. Only in the **malto-Au-Fe_xO_y (polymer)** fraction, the nanoparticles appear orderly aligned.*

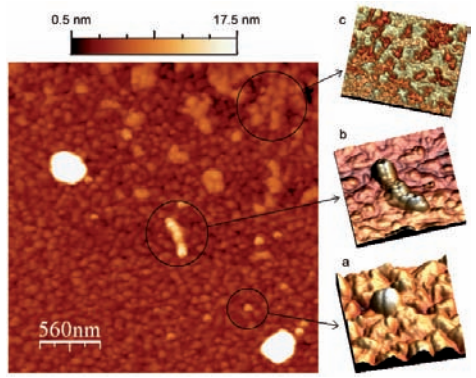

Figure 4. *The three different types of structures observed on gold with AFM: subunits as dimers **(a)**, subunits in complex formations **(b)** and self-assembled monolayers **(c)**.*

The amphiphilic character of the maltose neoglycolipid, with a hydrophilic head and a lipophilic spacer, may be the origin of the self-assembled arrangements in water solution. We think that the rows of aligned gold nanoparticles are produced through an encapsulation by self-assembled maltose neoglycolipid molecules that form a nanotube of organic material. Probably, the ability of the maltose neoglycolipids to form these micellar aggregates is due to carbohydrate self-interactions **[14]** between the maltose sugar residues as described in the crystal structure of the maltose disaccharide **[15]**. A sketch of the resulting tubular, micelle-like arrangement of maltose neoglycolipids containing Au-Fe_xO_y nanoparticles inside is shown in Figure 3.

Given that preliminary atomic force microscopy (AFM) analysis of ***malto*-Au-Fe_xO_y (polymer)** on mica seemed to confirm this encapsulation, we further explored the nature of this new material by different AFM techniques. The deposition of a droplet of ***malto*-Au-Fe_xO_y (polymer)** solution on a gold evaporated surface resulted in the formation of different kinds of structures as shown in **Figure 4.** Round elongated structures that we will refer to as "subunits" were often observed as dimers (**Figure 4a**). Also more complex formations like the one shown in **Figure 4b** were observed. A self-assembled monolayer (SAM) of the neoglycolipid appeared covering large portions of the gold surface area (**Figure 4c**). This monolayer consists of an excess of neoglycolipid molecules. As expected, the SAM shows a surface roughness similar to the gold grains underneath.

Figure 5 page 12 shows images of the complex formation of subunits in detail. As can be observed in the insets of the topographical image of **Figure 5a**, the subunits present typical dimensions of 65nm in length and 40nm in width. These subunits are interpreted as a set of cylindrical micelles consisting of a core of

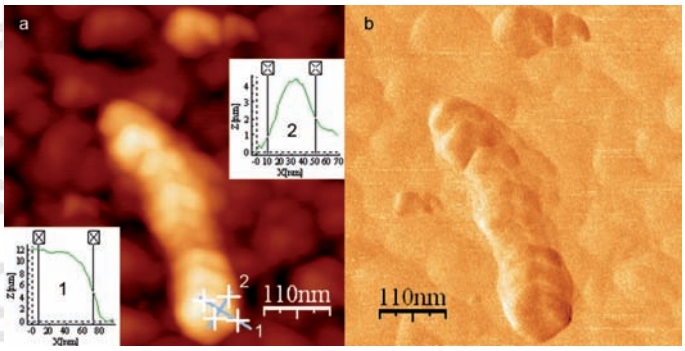

Figure 5. *Topographic* ***(a)*** *and phase* ***(b)*** *images of complex structure found on gold surfaces. The mean dimensions of the subunits found were about 65 x 40nm (example profiles 1 and 2 shown in the insets).*

aligned gold nanoclusters and an envelope of maltose neoglycolipid, similar as the domains observed in TEM analysis (Fig. 3). The phase image in **Figure 5b** shows chemical contrast between the organic material and the gold grains, thus confirming that indeed different materials are imaged.

In conclusion, by means of TEM and AFM analysis we have observed that maltose glyconanoparticle conjugates adopt specific arrangements when adsorbed on gold. We propose a micellar model to explain this new supramolecular structure based on carbohydrate self-interactions between the sugar residues and the amphiphilic character of the maltose neoglycolipid.

Opto-magnetic detection of superparamagnetic Fe_3O_4 nanoparticles dimer formation in liquids

In this study biofunctionalized superparamagnetic nanoparticles **[16]** are used as ultrasensitive molecular nanoprobes for the detection of targeted biological objects. Among many other options of detection mechanisms of molecular recognition we explore a less investigated opto-magnetic detection method. An advantage of this method is its compatibility with an unmodified biological environment.

Nanoparticles in the solution will scatter polarized light of a laser beam with a wavelength of 530nm since the Rayleigh scattering mechanism is effective for particles much smaller than the wavelength of light. This scattering will be polarization dependent for elongated or dimeric/chain aggregates of nanoparticles. Molecular recognition between conjugated biofunctionalized magnetic nanoparticles will lead to the formation of dimers and the application of a magnetic field orthogonal to the direction of light propagation will induce an optical anisotropy detectable by very sensitive polarimetric detection methods. In our setup the magnetic field can be pulsed or rotating. **Figure 6** illustrates the evolution of the transmitted laser beam intensity for a pulsed magnetic field when dimers are present.

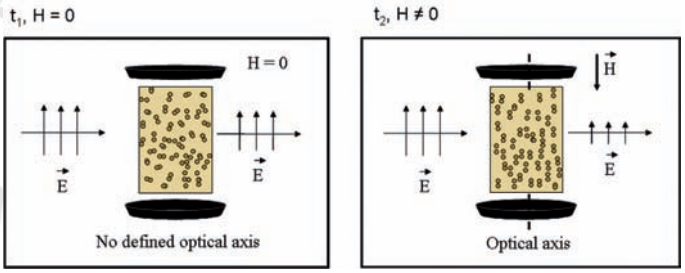

Figure 6. *Schematic of the difference of transmitted polarized light intensity for a pulsed magnetic field when dimers are present.*

Preliminary studies have been carried out employing Fe_3O_4 superparamagnetic nanoparticles with a diameter below 10nm coated with a surfactant to avoid agglomeration in water. Magnetic dipolar interactions between magnetic moments induced by a sufficiently large magnetic field will lead also to the formation of dimers that can be detected by polarized light. For sufficiently small superparamagnetic nanoparticles, for which Neel relaxation will dominate, dimer formation is reversibly controlled by the opposing effects of thermal agitation and attractive magnetic interactions.

In this work the optical polarization is analyzed for a rotating as well as a pulsed magnetic field, varying input parameters such as the strength and frequency of the magnetic field as well as the concentration of the nanoparticles in solution. In **Figure 7** the lock-in amplitude vs. the frequency of the rotating magnetic field is shown (the field strength is 4kA/m). A cut-off frequency of 20Hz characteristic of the dimers rotation dynamics can be identified.

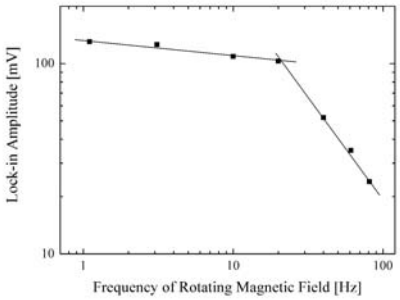

Figure 7. *Lock-in amplitude vs. frequency of the rotating magnetic field with a field strength of 4 kA/m. A cut-off frequency of 20 Hz characteristic of the dimers can be identified.*

The Brownian relaxation time of the particles when switching off the magnetic field can be extracted from the optical signal evolution. From this the hydrodynamic diameter of the particle can be derived, knowing the viscosity of the solution **[17]**. The hydrodynamic diameter can also be extracted from the phase lag between an applied rotating magnetic field and the optical signal.

Other experiments have been performed in liquid confined in micro-cavities of agarose. **Figure 8** shows a detail of the signal evolution for particles confined in these microcavities, applying a pulsed magnetic field of 2.5 kA/m. An

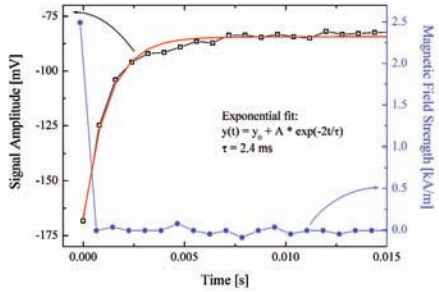

Figure 8. *Detail of the signal evolution for a pulsed magnetic field of 2.5kA/m. An exponential fit to the relaxation signal yields the characteristic relaxation time of the nanoparticles from which the hydrodynamic radius can be derived.*

NANOTECHNOLOGY

Raith

INNOVATIVE SOLUTIONS FOR NANOFABRICATION AND SEMICONDUCTOR NAVIGATION

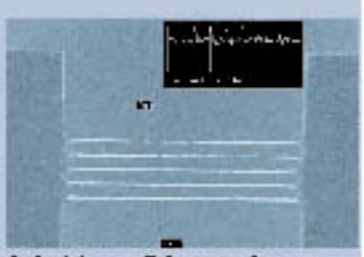

Sub 10 nm lithography

E-beam deposition

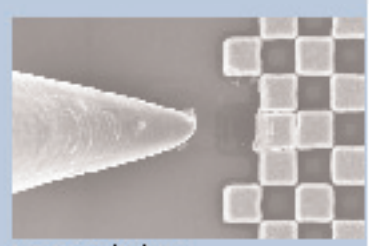

Nano Sokoban

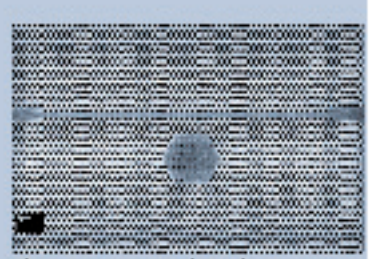

Photonic crystal with proximity effect correction

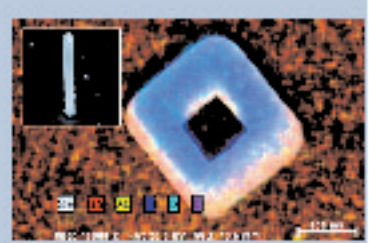

X-ray analytics

Ultra high resolution electron beam lithography and nano engineering workstation

eLiNE

...Nano metrology
...Nanoscale imaging
...EDX-chemical analysis
...Electron beam etching
...Electrical and mechanical probing
...Electron Beam Induced Deposition (EBID)

Upgrade your SEM / FIB to a nanolithography system

benefiting from a reliable modular attachment concept

ELPHY™ *PLus*

The advanced lithography system.....

ELPHY™ *Quantum*

The universal lithography attachment.....

Laser Interferometer Stage

The ultimate positioning tool.....

exponential fit to the relaxation signal yields a characteristic relaxation time of 2.4ms from which the hydrodynamic diameter of the particles can be extracted.

We conclude that the optomagnetic detection method is sufficiently sensitive to detect dimer formation by molecular interactions and appropiate to study nanoparticles dynamics in biologically relevant media.

Acknowledgements

This work has been funded by the Ministry of Education and Science (MEC) of Spain, projects NAN2004-09125-C07-02, CTQ2005-07993-C0202/BQU, the CSIC project PIF 200550F0172 and project Profit bioSense FIT-010000-2006-98 with the company Progenika Biopharma S.A.. M.L. acknowledges financial support from the MEC through the Ramón y Cajal program. M.F. and M.K. acknowledge financial support from a FPU grant and an I3P grant, respectively.

References

[1] a) J. M. de la Fuente, A. G. Barrientos T. C. Rojas, J. Rojo, J. Cañada, A. Fernandez, S. Penadés, **Angew. Chem. Int. J. 40, 2258-2261 (2001)**; b) A. G. Barrientos, J. M. De la Fuente, T. C. Rojas, A. Fernández, and S. Penadés, **Chem. Eur. J. 9, 1909-1921 (2003).**

[2] P. Crespo, R. Litrán, T. C. Rojas, M. Multigner, J. M. De la Fuente, J. C. Sánchez-López, M. A. Gracía, A. Hernando, S. Penadés and A. Fernández, **Phys. Rev. Lett. 93, 08724, (2004).**

[3] I. Brigger, C. Dubernet and P. Couvreur, **Adv. Drug. Rev. 54, 631, (2002).**

[4] J.W.M. Bulte, T. Douglas, B. Witwer, S.-C. Zhang, E. Strable. B.K. Lewis, H. Zywicke, B. Miller, P. van Gelderen, B.M. Moskowitz, I.D. Duncan and J.A. Frank, **Nat. Biotechnology, 19, 1141, (2001).**

[5] C.C. Berry and A.S.G. Curtis, **J. Phys. D: Appl. Phys. 36, R198, (2003).**

[6] V. A. Bloomfield, **Curr. Opin. Struct. Biol. 6, 334–341 (1996).**

[7] D. D. Dunlap, A. Maggi, M. R. Somia, L. Monaco, **Nucleic Acids Res. 25, 3095–3101 (1997).**

[8] a) E. Mastrobattista, M. A. van der Aa, W. E. Hennink, D. J. Crommelin, **Nat. Rev. Drug Discov. 5, 115–121 (2006).** b) A. Ragusa, I. Garcia, S. Penadés, **IEEE T on Nanobiosci. 6, 4, 319-330 (2007).**

[9] S. Zhang, Y. Xu, B. Wang, W. Qiao, D. Liu, Z. Li, **J. Control. Release 100, 165–180 (2004).**

[10] Z. P. Xu, Q. H. Zeng, G. Q. Lu, A. B. Yu, **Chemical Engineering Science 61, 1027–1040 (2006).**

[11] P. Eaton, A. Ragusa, C. Clavel, C. T. Rojas, P. Graham, R. V. Durán, S. Penadés, **IEEE T on Nanobiosci. 6, 4, 309-317 (2007).**

[12] I. Horcas, R. Fernández, J. M. Gómez-Rodríguez, J. Colchero, J. Gómez-Herrero and A. M. Baro, **Rev. Sci. Instrum. 78, 013705 (2007).**

[13] J. M. de la Fuente, D. Alcántara, P. Eaton, P. Crespo, T. C. Rojas, A. Fernández, A. Hernando, and S. Penadés, **J. Phys. Chem. B 110, 13021-13028 (2006).**

[14] J. Rojo, J. C. Morales, S. Penadés, **Topics Curr. Chem. 218, 45-92 (2002).**

[15] F. Takusagawa, R. A. Jacobson, **Acta Crystallogr. B34, 213-218 (1978).**

[16] I. García, J. Gallo, S. Penadés, **unpublished results.**

[17] E. Romanus, C. Groß, G. Glöckl, P. Weber, W. Weitschies, **J. Magn. Magn. Mater. 252, 384 (2002).**

Advertisement

NanoMEGAS has been created in 2004 by a team of scientists with expertise in electron crystallography

NanoMEGAS
Advanced Tools for electron diffraction

Our products are dedicated to help the TEM user (100-400 kv) to find in an easy way the true structure (crystal parameters, symmetry and atomic positions) of nanomaterials that are otherwise impossible to determine by X-ray diffractometry or high resolution TEM microscopy.

Our product **"spinning star"** takes control of the electron beam in a TEM and performs precession of a beam (Vincent- Midgley technique) in a way that one can obtain almost "kinematical" diffraction patterns.

A special dedicated software (**ELD-Emap**) can read and measure in automatic way intensities of ED patterns obtained with **"spinning star"**.

Spinning Star: Automatic Determination of Crystal Symmetry (K3Nb12O31F crystal)

PRECESSION OFF
1786 reflexions

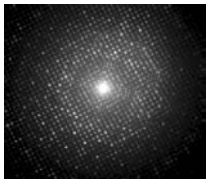

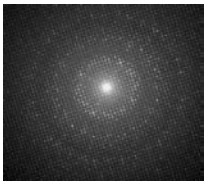

PRECESSION ON
3367 reflexions

NanoMEGAS SPRL
Boulevard Edmond Machtens 79; B-1080 Brussels (Belgium)
Email : info@nanomegas.com / http://www.nanomegas.com

Magneto-plasmonic materials: tuning magneto-optics with plasmons

G. Armelles, A. Cebollada, A. García-Martín, J.M. García-Martín, J.V. Anguita, J.B. González-Díaz, J.F. Torrado and E. Ferreiro*

Instituto de Microelectrónica de Madrid, Consejo Superior de Investigaciones Científicas, C/ Isaac Newton 8 (PTM) 28760 Tres Cantos, Spain

**antonio@imm.cnm.csic.es*

Introduction

During the last decades we have witnessed the development of a new branch in optics: plasmon optics or plasmonics **[1]**. This comes from the need to develop optical components in the nanoscale and to overcome the restriction imposed by the diffraction limit. Plasmonics has already given rise to novel devices, e.g. those based on the so-called supertransmission phenomenon **[2]** or on the properties of discrete plasmonic elements **[3]**. However, in order to achieve the same state as conventional optics it will be necessary to produce active materials. These active materials are, by definition, those whose optical properties can be controlled by an external agent. This external agent can be temperature, pressure, an electric field or a magnetic field, to name a few. Here we will concentrate on the magnetic field effects on the plasmon properties and on the reciprocal effect that plasmon excitation has over the magneto-optical response. Therefore, we will review our recent work on the combination of plasmons and magneto-optical (MO) activity. The first system will be made of a nanostructured ferromagnetic (thus having MO activity) metal (so it supports plasmons). More explicitly, it will be an ordered array of nickel wires, and we will show that the excitation of a plasmon running along the wire gives rise to an enhancement of the magneto-optical response **[4]**. Since the use of plain ferromagnetic metals is not good enough due to their broad plasmon resonance, it is necessary to go a step further. The second system is a continuous film made of a combination of magneto-optically active and noble plasmonic materials, presenting simultaneously well defined propagating surface plasmon polariton (SPP) resonances and MO activity which gives rise to systems with enhanced optical and MO responses. For instance, it has been shown that the MO response of Au/Co/Au trilayered systems can be enhanced when its surface plasmon resonance is excited **[5]**, enabling to develop new high sensitivity biosensors **[6]**. It has also been demonstrated that an applied magnetic field modifies the propagation vector of the plasmon in continuous films **[7]**. The third system shows that a discrete, nanostructured system exhibiting localized surface plasmon resonances (LSPR) may possess a mayor advantage with respect to continuous structures: the strong localization of the electromagnetic field associated to these resonances which might lead to a noticeable enhancement in the MO properties **[8]**, and could be exploited to make such a system become a promising candidate for the development of high spatial specificity magneto-plasmonic sensing devices.

Ferromagnetic metallic nanostructures

We will now describe the dependence of the magneto-optical properties on the size and on the dielectric environment of a system consisting on Ni nanowires embedded in an alumina matrix. This system presents interesting effects, such as an enhancement of the magneto-optical Kerr rotation, whose origin is a surface plasmon resonance of the Ni nanowires, its spectral position depending on the wire diameter **[4]**. In addition, it will be shown that the Kerr rotation spectrum depends on the local dielectric environment.

To that end we have used the MO Kerr effect in polar configuration, i.e. applying a magnetic field perpendicular to the matrix (therefore along the nanowires´axis) and measuring the light reflected by the magnetized sample, in particular the rotation of the polarization plane with respect to the incident linearly polarized light. **Figure FM1** shows the Kerr rotation spectrum for two different samples (A and B from now on) consisting in a hexagonal array of 5μm long Ni nanowires with a radius of 40nm and 180nm in alumina with an 105nm and 500nm pitch, as filled and open circles respectively. The continuous line represents the Kerr rotation of bulk Ni. For sample A we can clearly observe two distinct spectral regimes, below and above 2.5eV respectively. In the low energy regime the Kerr rotation is smaller than that of nickel bulk (basically proportional to the Ni concentration). However, beyond that point the Kerr rotation for the nanostructured sample becomes

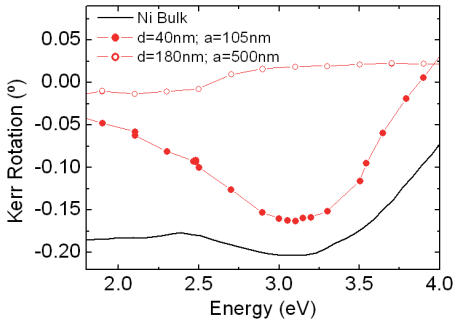

Figure FM1. *Kerr rotation spectrum of an array of nanowires with d=40nm and a=105nm (filled symbols) and d=180 and a=500nm (open symbols). The continuous line represents the Kerr rotation of nickel bulk. The enhancement of the rotation around 3eV is clearly visible for the first array.*

equivalent to that of bulk Ni, meaning that for this energy range it is possible to obtain a big effect despite having a smaller amount of magneto-optically active material. For the other sample the results are depicted as open circles in **Fig. FM1**, and we can see how the signal is significantly smaller than for Ni bulk in the whole spectral range covered, in this case being the nanostructure-to-bulk ratio in close relation with the nickel percen-tage. This indicates that the Kerr spectrum strongly depends on the diameter and separation of the motives.

In order to unravel the origin we now theoretically analyze the enhancement and its characteristics using a Scattering Matrix Method (SMM) adapted to be able to consider magneto-optical effects **[9]** to obtain an exact description of the wave propagation along the nanostructured material. In **Figure FM2 page16** (a) and (b) we present the result of numerical simulations for the Kerr spectra of nickel wires of three different diameters, namely 40, 80 and 125nm, adjusting the lattice parameter so that the

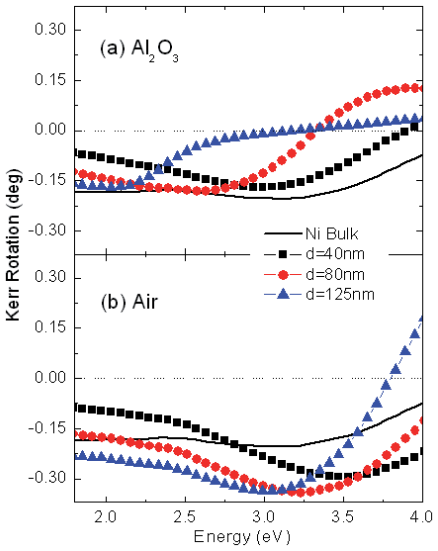

Figure FM2. *Theoretical Kerr rotation spectra for arrays of nickel nanowires with different diameters, keeping the nickel concentration constant, in.* ***(a)*** *embedded in alumina and in* ***(b)*** *air. The spectra appear red-shifted as the diameter of the wires increases. This red-shift also occurs for wires of equivalent diameter when the refractive index of the host increases. Despite that the nickel concentration is always around 18% the rotation is of the order (alumina) or even higher (air) than that of the bulk material. Adapted from J.B. González-Díaz et al. in* ***[4].***

nickel concentration remains constant (close to 18% as in the experimental case), in two different backgrounds: alumina (a) with n=1.7 and air (b) with n=1.

These simulations reveal that, for both environments, the region with enhanced Kerr rotation experiments a red-shift when the diameter of the wires increases. In the case of Ni nanowires embedded in air, the region is located in the ultraviolet energy range, shifting from 3.6eV to 3.2eV as we increase the diameter from 40nm to 125nm. Furthermore, when the matrix is alumina, the energetic position or the region is lower than that for the same diameter wires in air, indicating also a red-shift as a function of the refractive index of the environment. In addition, despite the fact that the amount of Ni in the nanowire layers is only about 18%, the intensity of the Kerr rotation of the system is either similar (alumina matrix) or even larger (air matrix) than that of a continuous Ni film. All these facts points to a plasmon-like excitation travelling along the wires as the origin of the enhancement of the Kerr signal.

Au/Co/Au films

We have discussed above the MO properties of a ferromagnetic metal. However, for magnetoplasmonic applications, the use of plain ferromagnetic metals is not good enough due to their broad plasmon resonance, as can be seen on **Figure F1 page 17**. These calculated curves have been obtained using a transfer matrix formalism assuming a Kreschmann configuration that couples the incident light to a SPP: firstly there is a peak corresponding to the total reflection condition, and then the reflected intensity reaches a minimum when the SPP excitation takes place. It can be observed that the width of such re-

Advertisement

SCHAEFER

www.schaefer-tec.com

SCHAEFER Techniques
1, rue du Ruisseau Blanc
Centre d'Activité de Lunezy
F-91620 Nozay

Telephon: +33 (0) 1 64 49 63 50
Telefax: +33 (0) 1 69 01 12 05
E-Mail: info@schaefer-tech.com
Web : www.schaefer-tech.com

NEW Instruments for New Challenges !

Scanning Probe Microscopes
Modular & Compact System

Nanosurf, easyScan 2

Nanoparticle Analysis
Individual & Real Time Detection

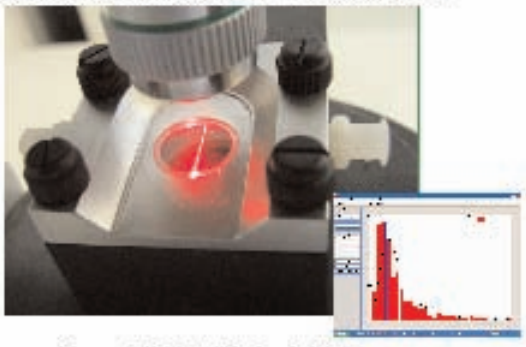

NanoSight, Halo LM10

We also represent the following companies, please contact us for further information :

- RHK for UHV STM/AFM and Cryogenic SPM
- QUESANT for AFM and STM
- MIKROMASCH for AFM tips and gratings
- KRATOS for XPS instrumentation
- OCI for LEED and AES
- FOGALE for optical Profilers
- ALICONA for Infinite Focus Microscope and MicroX
- HASTINGS for Vacuum and Gas Flow measurement
- HUNTINGTON for Vacuum Components

... and many other products in the field of Vacuum , Magnetism , Thin Film and Cryogenics

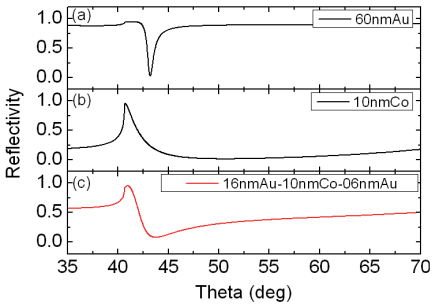

Figure F1. *Calculated angular variation of the reflectivity in the Kreschmann configuration for the following thin films assuming a glass substrate:* ***(a)*** *Au film 60nm thick ,* ***(b)*** *Co film 10nm thick, and* ***(c)*** *Au 6nm/Co 10nm/Au 16nm trilayer.*

sonance minimum is much larger in Co than in Au, due to the high optical absorption of the former. In order to obtain at the same time a reasonable width in the reflectivity minimum and MO activity using low magnetic field values, noble metals and ferromagnetic metals must be combined, for instance in the form of multilayers as in the pioneer work of Hermann et al. **[5].**

In our case, we have prepared a series of 6nm Au/Co/16 nm Au trilayers grown onto glass substrates by means of molecular beam epitaxy, and the Co thickness has been varied between 0 and 9 nm. To excite the SPP in these structures we have used the Kretschmann configuration, and the MO properties with and without SPP excitation have been analyzed using the MO Kerr effect in transversal configuration, i.e. applying a magnetic field in the plane of the sample and perpendicular to the plane of incidence of the linearly polarized light, measuring the reflected light intensity with a Si photodiode which has a p-oriented polarizer in front of it. The transverse Kerr activity is the normalized magnetic field induced variation of the reflectivity, $\Delta R_{pp}/R_{pp}$, *where* $\Delta R_{pp}(m_y) = R_{pp}(+1) - R_{pp}(-1)$, and m_y is the *y* component of the normalized magnetization $m_y = M_y/M_s$, M_s being the saturation magnetization of the Co layer. **Figure F2** shows the transverse Kerr activity with and without SPP excitation for the sample with a specific Co thickness of 7.7nm: in the absence of SPP excitation, the activity exhibits a smooth featureless evolution, in clear contrast with the behaviour when the SPP is excited. The latter situation reveals a significant structure for incident angle in the range of 40°- 46°, reaching a maximum activity that is twenty times larger than that obtained without SPP excitation. It can be probed that the SPP wave vector depends linearly on the *y* component of the magnetization. Therefore, the angle where the in-plane wave vector of the incident light matches the wave vector of the SPP of the layers (i.e., the reflectivity is minimum) will also depend on the *y* component of the magnetization. Thus, the transverse Kerr activity is related to the derivative of the reflectivity with respect to the SPP wave vector; in other words to $(\delta R_{pp}/\delta\theta)$ $(\Delta\theta R_{pp})$, where $\Delta\theta(m_y) = \theta_{min}(+1)\theta_{min}(-1)$ is the angular shift of the reflectivity minimum when the magnetization is reversed, and represents the variation of the SPP wave vector induced by the change in magnetization direction. This fact is illustrated in Figure F2 comparing (b) and (c), which are pretty similar with the exception of the small dip in the derivative of the reflectivity at 40deg that corresponds to the onset of total internal reflection.

This represents experimental evidence of nonreciprocal magnetic field induced effects in the propagation properties of SPP in Au/Co/Au. This effect is observed at low magnetic fields and depends on the magnetization of the Co layer and can be tuned by varying the Co layer thickness.

Au/Co/Au nanostructures

Complex onion-like nanoparticles made of noble metals and ferromagnets that exhibit LSPR have been obtained using different chemical methods **[10]**. However, no MO activity has been reported so far. The nanostructures studied in our case are stacked Au/Co/Au nanodisks that do exhibit simultaneous LSPR, magnetic, and MO properties. These nanostructures have been prepared by means of sputtering of trilayer films onto glass substrates and subsequent colloidal lithography, i.e. an array of self assembled latex spheres with short range order acted as masks for Ar-ion beam etching. The composition of the films was kept constant (6nm of Au on top/ 10nm of Co/ 16nm of Au) and the nanodisk size was controlled by using latex spheres with different diameter (60, 75 and 110nm). **Figure N1** shows an atomic force microscopy (AFM) image of the nanodisks obtained using latex spheres of 110nm diameter. The resulting nanostructures have a mountainlike shape that is mainly due to the leftovers of the latex spheres, therefore explaining the difference between the nominal height of the nanodisks and that obtained by AFM, which is always higher than 32nm.

The nanostructuration gives rise to strong changes in the optical absorption properties of the system, as shown in

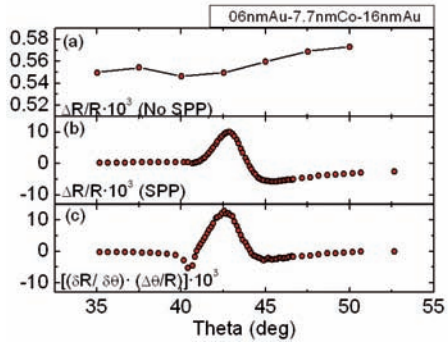

Figure F2. *(a)-(b) Transverse Kerr activity for a Au/Co/Au trilayer* ***(a)*** *without SPP excitation, and* ***(b)*** *with SPP excitation.* ***(c)*** *Derivative of the reflectivity with SPP excitation.*

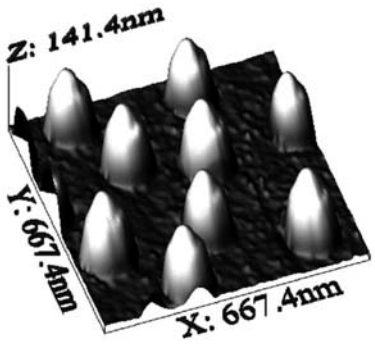

Figure N1. *AFM image of Au/Co/Au nanodisks with 110nm diameter.*

the absorption spectra of the samples shown in **Figure N2**, where the corresponding curve of a sample containing Au nanodisks of 60nm diameter and 32nm height has been included for comparison. The spectra of all the samples is characterized by a peak associated with the LSPR. Compared to the Au 60nm diameter disks, the LSPR peak of the Au/Co/Au disks broadens and is shifted toward higher energy. Both the shift and the broadenings of the LSPR peak induced by introducing Co instead of pure Au have previously been observed in core/shell nanoparticles made of ferromagnetic and noble metals. The shift depends on the actual structure of the nano-objects, since both blue- and red-shifts have been observed for different systems **[10]**. However, the broadening of the LSPR peak was always observed and has been ascribed to the high absorption of Co. More interestingly, the peak of the Au/Co/Au nanodisks shift towards lower energy as the disk diameter is increased (see inset of Figure N2, where the energetic position of the absorption peak for the different disks is depicted). This behavior is similar to that observed for pure noble metal nanoparticles and is a clear indication of its plasmonic origin.

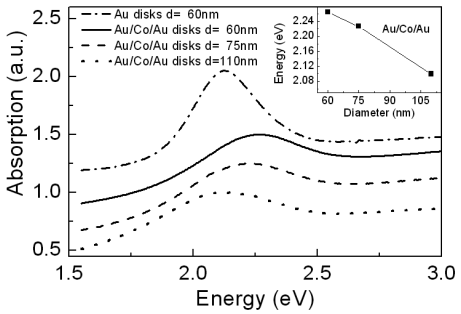

Figure N2. *Absorption spectra of several Au/CoAu nanodisk samples with different diameter and for a Au nanodisk sample for the sake of comparison. In the inset, the energy position of the extinction peaks as a function of the diameter is shown.*

Noteworthy, the excitation of the LSPR in the nanodisks affects their MO response, leading to a net enhancement of the MO signal. To illustrate this effect we have used the MO Kerr effect in polar configuration, i.e. applying a magnetic field perpendicular to the nanodisks and measuring the light reflected by the magnetized sample, in particular the rotation of the polarization plane and the change in the ellipticity state with respect to the incident linearly polarized light. **Figure N3** shows the total polar Kerr activity (defined as the $\phi^2 = |\theta + i\,\phi|^2$, where θ is the Kerr rotation and ϕ is the Kerr ellipticity) of the 60 and 110nm diameter nanodisks normalized to that of a continuous Au/Co/film with the same composition and amount of material (i.e. multiplied by the filling fraction f). Two facts must be noticed: (i) such activity exhibits a peak located in the same energetic region than the LSPR, and the displacement of the peak follows the same behaviour than that of the LSPR absorption peak when the disk diameter is increased (it goes to lower energy); (ii) there is an enhancement on the MO activity of the nanodisk compared to that of the continuous film (normalized activity larger than one), which indicates that the excitation of the LSPR led to an enhancement in the MO response.

To the best of our knowledge, this is the first demonstration of a plasmonic nanostructure that can be controlled by an external magnetic field.

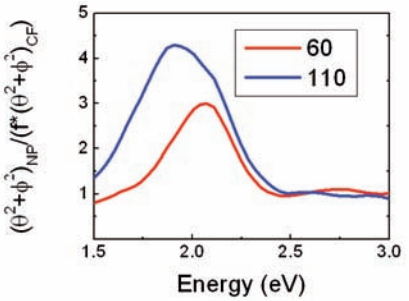

Figure N3. *Normalized polar Kerr activity for Au/Co/Au nanodisks with 60 and 110nm diameter.*

Summary

To sum up, we have shown that the combination of plasmonic and magneto-optically active materials can be the ideal candidates to develop "active plasmon optics", the heir of conventional optics at the nanoscale. We have not only shown that the MO activity can be enhanced by the excitation of a plasmon, key element in the development of a new generation of biosensors and in magneto-optical information storage, but also that the propagation of the plasmon itself can be modified by the presence of a magnetic field, key element in the design of plasmon-based telecommunication applications.

Acknowledgments

The work described in here could not have been done without the benefit of long-standing collaborations: *Ferromagnetic metallic wires:* D. Navas and M. Vázquez, Instituto de Ciencia de Materiales de Madrid (Spain); K. Nielsch, U. Hamburg (Germany); U. Gösele Max-Planck-Institute of Microstructure Physics (Germany); and R.B. Wehrspohn Fraunhofer-Institut für Werkstoffmechanik Halle, (Germany); *Au/Co/Au films:* R. A. Lukaszew and J. R. Skuza, University of Toledo (USA); D. P. Kumah and R. Clarke University of Michigan (USA); *Au/Co/Au nanostructures:* B. Sepúlveda, Y. Alaverdyan, and. M. Käll, Chalmers University of Technology (Sweden).

We also acknowledge financial support from Spanish Ministry of Science and Education (NAN2004-09195-C04 and MAT2005-05524-C02-01), Comunidad de Madrid (S-0505/MAT/0194 and Microseres), CSIC (Refs. 200650I130 and 200650I032) and EU (NoE-Phoremost).

References

[1] S. A. Maier, *"Plasmonics: Fundamentals and Applications"*, **Springer (2007)**

[2] T.W. Ebbesen et al., **Nature 391, (1998) 667**

[3] J. Cesario, et al., **Opt. Express 15, 1(2007)0533**, L. Liz-Marzan, **Langmuir. 22, (2006) 32**

[4] S. Melle et al., **Appl. Phys. Lett. 83, (2003) 4547**; J.B. Gonzalez-Diaz et al., **Adv. Mat.. 76, (2007) 153402**

[5] Hermann et al., **Phys. Rev B 64,, (2001) 235422**

[6] B. Sepúlveda et al., **Oppt Lett.31, (2006) 1085**

[7] J.B. Gonzalez-Diaz et al., **Phys. Rev. B. 76, (2007) 153402.**

[8] J.B. Gonzalez-Diaz et al., **Small 4, (2008) 202.**

[9] A. Garcia-Martin, G. Armelles, and S. Pereira, **Phys. Rev. B 71,(2005) 205116.**

[10] N. S. Sobal et al., **Nano Letters 2, (2002) 621**; Z.Ban et al **J. Mater. Chem 15, (2005) 4660**; J. Zhang et al., **J. Phys. Chem B 110, (2006) 7122**; S. Mandal et al., **J. Mater. Chem 17 , (2007) 372**

A WIDE RANGE OF VERSATILE NANO TECHNOLOGY SOLUTIONS

Enjoy Productivity, Reliability and Precision

Carl Zeiss SMT
Nano Technology Systems Division
info-nts@smt.zeiss.com
www.smt.zeiss.com/nts

Enabling the Nano-Age World®

ZEISS

NANO Vacancies - http://www.phantomsnet.net/Resources/jobs.php

PostDoctoral Position (CEA Grenoble, France): *"Electrical Characterization and Physical Modeling of Chalcogenide Materials for Application to Sub-45nm Embedded Phase-Change Non-Volatile Memories"*

Main objectives of this postdoc position will be the electrical characterization and physical modeling of chalcogenide materials for application to sub-45nm embedded Phase-Change Non-Volatile Memories.
The work will be performed at LETI-MINATEC (micro and nanoelectronics laboratories LSCDP and LNDE)

The deadline for submitting applications is June 18, 2008
For further information about the position, please contact: L. Perniola (**luca.perniola@cea.fr**)

PostDoctoral Position (University of Alicante, Spain): *"Solid quantum-dot sensitized nanostructured semiconductor/organic solar cells."*

The research will involve the synthesis of oxide nanostructures and QDs by wet methods, as well as preparing and characterizing solar cells using both electrochemical and spectroscopic methods.

The deadline for submitting applications is June 14, 2008
For further information about the position, please contact: Roberto Gómez (**Roberto.Gomez@ua.es**)

PostDoctoral Position (Catalan Institute of Nanotechnology, Spain): *"Light scattering and diffusive transport to investigate phonons in nanostructures"*

The postdoctoral position has as main task to contribute to the understanding of thermal transport in the nanometer scale by using mainly inelastic light (Raman) scattering and, to a leeser degree, diffusive transport technique. The work is in close collaboration with the modelling team of the NANOPACK project.

The deadline for submitting applications is April 30, 2008
Applications, consisting of a CV, the name and contact details of three referees, mentioning the position reference nº in the subject line, may be sent to: Clivia M. Sotomayor Torres (**clivia.sotomayor.icn@uab.es**)

PhD Positions (2) (Instituto de Optica, CSIC, Spain): *"Laser processing of materials, ultrashort laser pulses technology, nanotechnology, materials for integrated optical devices.laser-matter interaction"*

The Laser Processing Group of the Optics Institute of the Spanish National Research Council (CSIC) offers 2 PhD contracts for 1 year with possibility for extension up to 4 years, to perform research work in collaboration with groups of other EU countries in the frame of projects funded by both Spanish agencies as well as Frame Program of EU.
The PhD Thesis will be related to the following topics laser processing of materials, ultrashort laser pulses technology, nanotechnology, materials for integrated optical devices, laser-matter interaction, nanotechnology, non-linear optics and waveguide integrated optical devices.

The deadline for submitting applications is May 10, 2008
For further information about the position, please contact: Rosalía Serna (**rserna@io.cfmac.csic.es**)

PhD Position (Institute for Bioengineering of Catalonia (IBEC), Spain): *"Single (bio)molecule detection and analysis working at the intersection between Physics and Biology"*

The BioNanoPhotonics group at the IBEC focuses its research in the field of single (bio)molecule detection and analysis working at the intersection between Physics and Biology. The group is currently offering one research position at PhD level associated with an FPI grant from the Spanish Ministry of Education and Science.

The deadline for submitting applications is June 03, 2008
Applicants should send a covering letter stating their suitability for and reasons of interest in the position, together with a full CV, including the list of published work and contact details of referees by email at **jobs@ibec.pcb.ub.es** (**Ref.: Single Molecule**). For more information, please contact: Prof. M. F. Garcia-Parajo at **mgarcia@pcb.ub.es**

NANO Vacancies - http://www.phantomsnet.net/Resources/jobs.php

PhD Position (Universidad Autonoma de Madrid, Spain): *"Self-assembling of molecules at surfaces: Model systems for organic solar cells, organic transistors and organic magnets."*

The main goal of this project is to explore the self assembling process of organic molecules at surfaces in systems with technological applications. The work will imply the structural characterization of the surfaces with techniques as Atomic Force Microscopy (AFM) and Surface X-ray Diffraction (SXRD) in our lab and in european facilities.

The deadline for submitting applications is June 03, 2008
For further information about the position, please contact: Jesus Alvarez (**jesus.alvarez@uam.es**)

PostDoctoral Position (Laboratoire des Technologies de la Microélectronique - LTM, France): *"Development of plasma etching processes for microelectronics, the fabrication and study of nanomaterials and nanodevices, and the development of lithographies such as nanoimprint and simulation tools for optical lithography."*

The "Laboratoire des Technologies de la Microélectronique" (LTM) is an academic research laboratory depending on CNRS and Grenoble Universities, and hosted by CEA-LETI on the Minatec Site. Its main research activities are the development of plasma etching processes for microelectronics, the fabrication and study of nanomaterials and nanodevices, and the development of lithographies such as nanoimprint and simulation tools for optical lithography.

The deadline for submitting applications is May 25, 2008
For further information about the position, please contact: Cécile Gourgon (**cecile.gourgon@cea.fr**)

PhD Position (University of Murcia, Spain): *"An integrated approach of organic solar cells: from Nano to Macro"*

We offer the possibility to collaborate as a PhD student in the development and improvement of organic solar cells. The corresponding studies will be undertaken at the two relevant scales: the traditional macroscopic scale, which is the scale where the cells are fabricated and used, and the nanoscopic scale, which determines the physical and chemical processes on which solar energy conversion is based. Scanning force microscopy (SFM / AFM) will be a key tool in our studies.

The deadline for submitting applications is May 15, 2008
For further information about the position, please contact: Jaime Colchero (**colchero@um.es**)

PostDoctoral Position (Sevilla Microelectronics Institute, Spain): *"Preliminary unofficial announcement: Nanofet device modeling and system design"*

Targeting the development of computing solutions complementing logic functions based on CMOS, the main objective of the NABAB project consists of "demonstrating that it is possible to obtain useful computing functions as the result of a post-fabrication learning/adaptation process taking advantage of the rich functionality provided by interconnected nano devices".

The deadline for submitting applications is April 30, 2008
For further information about the position, please contact: Teresa Serrano-Gotarredona (**terese@imse.cnm.es**)

PhD Postion (INAC-CEA-GRENOBLE, France): *"Non-contact atomic force microscopy investigations of self-organized pi-conjugated molecular wires"*

To promote the self-assembly of pi-conjugated molecules into nano-wires, surface functionalization by a "buffer layer" of insulating silanes will be eventually required. In this case, the local conformation of the silane mono-layers will be studied at the sub-molecular level by NC-AFM prior to the deposition of the conjugated molecules. In the frame of our last developments in the field of organic field effect transistors, maste-ring the self-organization of molecular wires on SiO2 will allow to realize molecular-based devices, which local electro-nic transport under electrostatic doping will be probed by scanning Kelvin probe microscopy under UHV.

The deadline for submitting applications is June 30, 2008
Applications (to be sent at **benjamin.grevin@cea.fr**) should include a detailed curriculum vitae and a letter in which the applicant states her/his interests and experiences relevant to this project.

NANO Conferences http://www.phantomsnet.net/Resources/cc.php

(May 2008)

- **The fifty-second International Conference on electron, Ion, and Photon Beam technology and Nanofabrication (EIPBN2008).**
May 27-30, 2008. Hilton Portland & Executive Tower, Portland, Oregon (USA)
http://www.eipbn.org
NanoFabrication, NanoLithography

- **Hyper-Nano2008.**
May 26-28, 2008. Fodele, Crete (Greece)
http://users.auth.gr/~kkaratas/workshop/workshop.html
Theory & Modeling

- **International Workshop on Wearable Micro and Nanosystems for Personalised Health (phealth2008).**
May 21-23, 2008. Valencia (Spain)
http://www.phealth2008.com
Nanotechnologies

- **European Society for Precision Engineering and Nanotechnology conference.**
May 18-22, 2008. Kongresshaus Zurich (Switzerland)
http://www.zurich2008.euspen.eu
NanoMaterials, NanoFabrication, NanoMetrology & Standards

- **International Symposium on "Electron dynamics and electron mediated phenomena at surfaces: femto-chemistry and atto-physics" (Ultrafast2008).**
May 07-08, 2008. San Sebastian (Spain)
http://dipc.ehu.es/ws_presentacion.php?id=26
Theory & Modeling

NANO Conferences http://www.phantomsnet.net/Resources/cc.php

Course on Nanotechnology and Mathematics.
May 06-08, 2008. Santiago de Compostela (Spain)
http://nanomath.weebly.com
Theory & Modeling, Nanotechnologies

(June 2008)

International Conference on IC Design and Technology.
June 2-4, 2008. MINATEC-Grenoble, (France)
http://www.icicdt.org
Nanoelectronics

NanobioEurope2008.
June 09-13, 2008. Barcelona (Spain)
http://www.nanobio-europe2008.com
NanoBiotechnology, NanoMedicine

2nd International Conference on Advanced Nano Materials (ANM2008).
June 22-25, 2008. Aveiro (Portugal)
http://anm2008.web.ua.pt
NanoMaterials

MINATEC Crossroads2008.
June 23-27, 2008 Grenoble, (France)
http://www.minatec-crossroads.com
Nanoelectronics, Nanotechnologies

NANO News - http://www.phantomsnet.net/Resources/news.php

European Roadmap for Photonics and Nanotechnologies (27-03-2008)
http://www.ist-mona.org/roadmaps/default.asp
Photonics and Nanotechnologies are highly multi-disciplinary fields and two of the principal enabling technologies for the 21st century. They are key technology drivers for industry sectors such as information technologies, communication, biotechnologies, transport, and manufacturing. The MONA Roadmap identifies potential synergies between photonics/nanophotonics and nanomaterials/nanotechnologies. The challenge of mastering nano-electronics and nanophotonics science and technologies at an industrial scale is of utmost strategic importance for the competitiveness of the European industry in a global context.
Keywords: Nanophotonics & NanoOptoelectronics / Nanomaterials / Scientific Policy

Nanophotonic structures suitable for CMOS compatible technologies (26-03-2008)
http://www.nanowerk.com/spotlight/spotid=5062.php
Researchers in The Netherlands have demonstrated a method to etch arrays of nanopores in silicon with record depth-to-diameter ratios. These structures are suitable for nanophotonics and were made completely with CMOS compatible technologies, making integration of photonic structures in silicon chips feasible.
Keywords: Nanophotonics & NanoOptoelectronics

Electron spin and orbits in carbon nanotubes are coupled (26-03-2008)
http://www.physorg.com/news125767527.html
Cornell physicists have found that the spin of an electron in a carbon nanotube is coupled the electron's orbit. The finding means researchers will have to change the way they read out or change spin, but offers a new way to manipulate the spin, by manipulating the orbit
Keywords: Nanotubes .

Nanotechnology composite materials for next generation biomedical applications (25-03-2008)
http://www.nanowerk.com/spotlight/spotid=5043.php
A novel nanocomposite of carbon-nanotube-reinforced PMMA/HA is a demonstration of how nanomaterials will play an increasing role in the synthesis of next-generation biomedical applications.
Keywords: Nanotubes / Nanobiotechnology / Nanomedicine

Physicists Show Electrons Can Travel More Than 100 Times Faster in Graphene (24-03-2008)
https://www.newsdesk.umd.edu/scitech/release.cfm?ArticleID=1621
University of Maryland physicists have shown that in graphene the intrinsic limit to the mobility, a measure of how well a material conducts electricity, is higher than any other known material at room temperature.
Keywords: Nanomaterials

Nanophotonic switch device for routing light on a chip scale (17-03-2008)
http://www.physorg.com/news124988995.html
IBM scientists took another significant advance towards sending information inside a computer chip by using light pulses instead of electrons by building the world's tiniest nanophotonic switch.
Keywords: Nanophotonics & NanoOptoelectronics / Nanosensors & Nanodevices

Carbon Nanotubes Outperform Copper Nanowires as Interconnects (13-03-2008)
http://news.rpi.edu/update.do?artcenterkey=2412
Researchers at Rensselaer Polytechnic Institute have created a road map that brings academia and the semiconductor industry one step closer to realizing carbon nanotube interconnects, and alleviating the current bottleneck of information flow that is limiting the potential of computer chips in everything from personal computers to portable music players.
Keywords: Nanotubes / Theory and modelling

Applied Materials: Patterning Requires Innovative Metrology (29-02-2008)
http://www.semiconductor.net/article/CA6536275.html?nid=3572
Applied Materials concurrently held its 12th Annual Technology Forum with SPIE Advanced Lithography Conference in San Jose. Having "Reality Takes Shape: Patterning at 32 nm" as its theme, the wide-ranging event covered a number of subjects, not the least of which were the challenges faced by metrology.
Keywords: Nanometrology & Standards / Nanopatterning

Design and production of micro and nanostructured polymer substrates for cell culture applications

E. Martínez[1], C.A. Mills[1], A. Lagunas[1,2], M. Estévez[1], S. Rodríguez-Segui[1], J. Comelles[1], S. Oberhansl[1] and J. Samitier[1,2,3]*

[1]Nanobioengineering group, Institute for Bioengineering of Catalonia (IBEC), Josep Samitier 1-5, 08028 Barcelona, Spain.
[2]Networking Research Center on Bioengineering, Biomaterials and Nanomedicine (CIBER-BBN), Barcelona, Spain.
[3]Department of Electronics, University of Barcelona, c/ Martí i Franquès 1, 08028 Barcelona, Spain.

corresponding author: **emartinez@pcb.ub.es, Tel. +34 93 403 71 77*

Introduction

In vivo, cells interact with each other, thus triggering diverse intracellular processes that control cell development. Moreover, the cell surrounding environment, constituting the extra-cellular matrix (ECM) and soluble factors, causes cells to adapt and reprogram their intracellular apparatus. Cells can sense, then, topological, chemical and physical cues within the surrounding milieu. Indeed, it has been reported that mammalian cells respond to micro and nanostructures created on artificial surfaces **[1-3]**. Hence, artificial bio-functionalised substrates with nano and micropatterns might make cells develop through different pathways, depending on the substrate design, in a non-invasive approach; specifically controlling processes such as cell adhesion, survival, proliferation, migration and differentiation. The principle relies on genetic reprogramming via intracellular signalling pathways, due to specific reactions through customized nanostructured surfaces in contact with cell surface receptors.

Moreover, in recent years, the interest in the fundamental knowledge of cell-substrate interaction has increasingly grown as it is now recognized to play a key role in the differences observed in cell behaviour when comparing in vitro and in vivo culturing **[4]**. This appears, then, as a crucial factor for tissue engineering, drug development and regenerative medicine fields. As substrate topolography and biochemistry can be highly controllable factors, an understanding of these aspects will help in creating functional engineered tissues, as well as in the design of many implantable medical devices.

The main objective of our work is to apply novel micro and nanofabrication techniques and surface modification strategies to generate well-defined topographical and biochemical cues for cell culture. To achieve this goal, nanoembossing has been used to impart micro and nanostructures into polymer substrates, and their surface properties modified by micro-contact printing, nanoplotting and dip-pen nanolithography of ECM proteins, which are attached covalently to the surface. The modified surfaces are then used to study their influence on cell adhesion, morphology, proliferation and differentiation.

Keywords: microstructure, nanostructure, cell-surface interaction, micropattern, nanopattern polymer

Experimental

Polymer surfaces containing both chemical functionalisation patterned at the micro-scale and regular nano-topography have been produced for use in surface interaction studies with cells. The polymer-based surfaces are to be used in conjunction with optical analysis methods, such as confocal microscopy, where the cell surface interactions can be discerned.

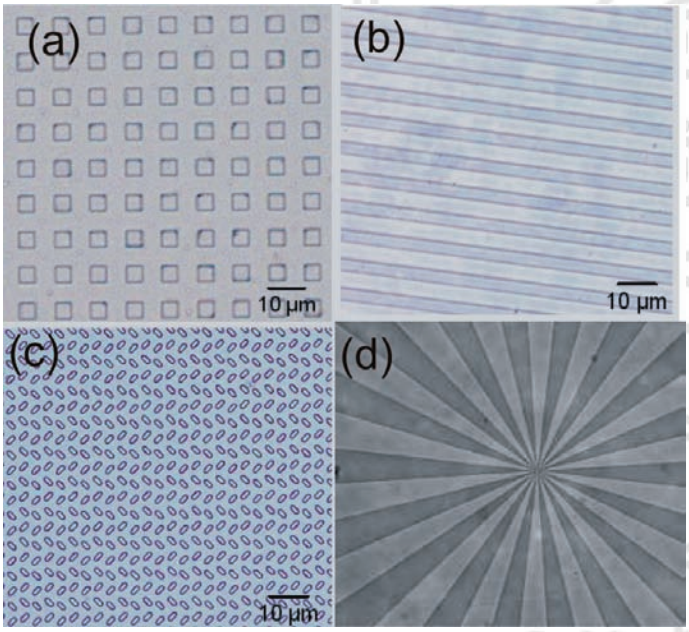

Figure 1. *Different geometries of microstructured substrates assayed in cell culture.* ***(a)*** *posts of 5µm in size,* ***(b)*** *lines of 5µm in size,* ***(c)*** *small structures 2µm in size and* ***(d)*** *star-like structure of 20µm in size (ending points of the picture). Samples (a) to (c) were realized in PMMA while sample (d) was performed in titanium dioxide composite material (courtesy of INM, Germany)*

Nanoembossing is achieved using nanoimprint lithography apparatus in biocompatible polymers such as poly(methyl methacrylate) (PMMA) **[5]** or titanium dioxide biocompatible composites (**Figure 1**). The PMMA was obtained in 125µm thick sheets (Goodfellow, UK) and used for the nanoembossing after rinsing the surfaces with isopropanol. Moulds for the nanoembossing were produced using conventional photolithography techniques combined with dry etching processes (microscale features) and focussed ion beam lithography or e-beam lithography (nanoscale features). The moulds were previously treated with a fluoroalkylsilane, (trichloro(tridecafluoro-octyl)-silane, for anti-adhesion purposes, so they can be reused after demoulding. Mould layout and thus, replica, were carefully designed to fit in a flexiPERM (Greiner Bio-One GmbH, Germany) cell culture system.

Micro/nanopatterning of biochemical factors were undertaken by a variety of techniques, including micro-contact printing using PDMS stamps, nanolitre non-contact drop delivery (nanoplotter) and dip pen nanolithography, performed using a dedicated AFM instrument. Methods for micro and nanocontact printing have been conveniently modified to maximize the lateral resolution by using liquid environments and/or PMMA moulds instead of the usual PDMS ones **[6,7]**.

Results and discussion

Results show that surface topography is instrumental in cell guidance and alignment processes (**Figure 2 page 26**), but it also greatly affects cell morphology, as cells can be elongated, spindle-shaped or more rounded depending

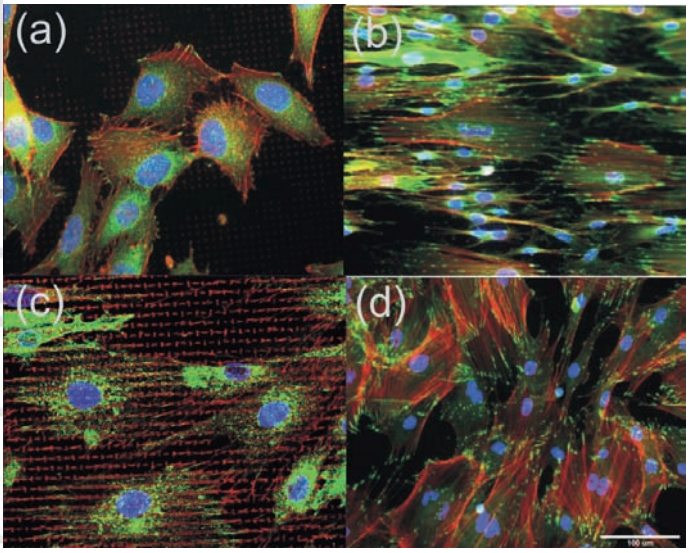

Figure 2. *Different morphologies adopted by rat mesenchymal stem cells after culture (3 days) in the substrates described in figure 1. Samples are immunologically stained as follows: nuclei in blue, focal contacts in green and actin filaments in red (figures* ***(b)*** *and* ***(d)****). In figures* ***(a)*** *and* ***(c)*** *the red staining, that marks the location of the topographical figure, corresponds to fibronectin.*

on surface structures. These geometrical parameters can be quantified depending on the topographical dimensions of the substrate features **[5]**. The different cell morphologies and cytoskeletal organization has been observed by scanning electron microscopy and confocal/fluorescence microscopy through the staining of the actin filaments.

Surface functionalisation with adhesion proteins such as fibronectin can be used to selectively attach and confine cells at specific surface locations, thus creating the structures called cellular microarrays. These microarrays, that can be constructed by the surface immobilisation of different types of biomolecules or combination of biomolecules can provide well known microenvironments to study cell behaviour and, in particular, cell differentiation. Our last results aim to establish the parameters for the culture and differentiation of mesenchymal stem cells on a microarray format **[8]**, as well as the techniques that can be used to order the biomolecules at different discrete positions in a substrate (**Figure 3**) **[9]**.

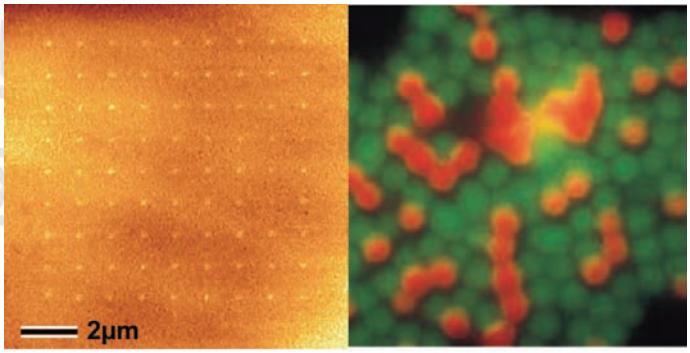

Figure 3. *Thiol-biotin dots (200nm in size) deposited on a gold surface by dip-pen nanolithography* ***(left)****. Latex beads (1µm in size) immobilized on a glass surface with different fluorophores (biomolecules)* ***(right)***

Conclusions

We have described different methodologies for the production of topographically structured and biochemically patterned polymer surfaces. Such surfaces are suitable for a number of applications, such as cell culture or the study of cell-substrate interactions at the micro and nanometer scale. With the techniques presented here, it is straightforward to envisage the next steps as the combination of chemical and structural patterning and the 3D structures to better mimic the in-vivo cellular molecular landscapes.

Acknowledgements

This work has been generated in the context of the CellPROM project, funded by the EC (contract No. NMP4-CT-2004-500039) and it reflects only the authors' views. The authors thank Drs. C. Moormann and T. Wahlbrink of AMO Gmb (Germany) for providing the moulds used for nanoembossing, Dr. S. Gerbes (INM, Germany) for providing the titanium dioxide nanoembossed materials, M. Funes (IBEC) for cell culturing and E. Engel (IBEC) for biological advice in the experiments performed.

References

[1] Dalby MJ, Gadegaard N, Riehle MO, Wilkinson CD, Curtis AS. *Investigating filopodia sensing using arrays of defined nano-pits down to 35 nm diameter in size.* **Int J Biochem Cell Biol 2004;36(10):2005-15**.

[2] Andersson AS, Backhed F, von Euler A, Richter-Dahlfors A, Sutherland D, Kasemo B. *Nanoscale features influence epithelial cell morphology and cytokine production.* **Biomater 2003;24(29);3427-36.**

[3] Miller DC, Thapa A, Haberstroh KM, Webster TJ. *Endothelial and vascular smooth muscle cell function on poly(lactic-coglycolic acid) with nano-structured surface features.* **Biomater 2004;25(1):53-61.**

[4] Flemming RG, Murphy CJ, Abrams GA, Goodman SL, Nealey PF, *Effects of synthetic micro and nanostructured surfaces on cell behaviour*, **Biomaterials 1999;20:573-588**

[5] Mills, C. A.; Fernandez, J. G.; Martinez, E.; Funes, M.; Engel, E.; Errachid, A.; Planell, J.; Samitier, **J. Small 2007, 3, 871**

[6] M. Pla-Roca, J. G. Fernandez, C.A. Mills, E. Martínez, J. Samitier, *Micro-/nano-patterning of proteins using a nanoimprint-based contact printing technique and high aspect ratio poly(methyl methacrylate) stamps*, **Langmuir 2007; 26**

[7] Bessueille F, Pla-Roca M, Mills CA, Martinez E, Samitier J, *Errachid A Submerged microcontact printing (SmuCP): an unconventional printing technique of thiols using high aspect ratio, elastomeric stamps*, **Langmuir 2005; 21(26):12060-3**

[8] Rodriguez-Segui SA, Pla-Roca M, Engel E, Planell, J.A., Martínez E. and Samitier J, *Customized cellular microarrays for mesenchymal stem cells studies*, **Langmuir (submitted)**

[9] Issle J, Pla-Roca M, Martinez E, Hartmann U, *Patterning of magnetic nanobeads on surfaces by PDMS stamp*, **Langmuir 2008 (in press)**

Mach V.

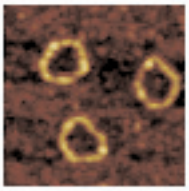

AFM image of mini-circle DNA with approximately 340 base pairs. 130nm x 130nm.

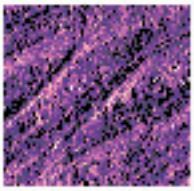

Unmineralized collagen fibrils of trabecular bone. 8.4µm x 8.4µm.

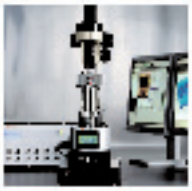

MultiMode V Atomic Force Microscope.

INTRODUCING di MULTIMODE V ATOMIC FORCE MICROSCOPE: THE FASTEST PATH TO PUBLICATION

Investigate nanoscale events at timescales previously inaccessible with NultiNode® V's high speed data capture. Acquire 8 images simultaneously for faster time to data; utilize Nanoscript™ open architecture for control of your NanoBio experiments. All of this plus our new Easy-AFM make the NultiNode V AFM the fastest path to publication. Find out more about the latest version of the world's highest performance and most published AFM. Visit *www.* veeco.com/multimodev today or call:

Cambridge, UK	Int + 44 (0) 1954 233900
Dourdan, F	Int + 33 (0) 1645 93520
Nannheim, D	Int + 49 (0) 6218 42100
Breda, NL	Int + 31 (0) 7652 44850

Veeco

Solutions for a nanoscale world.™

Easy to scale-up preparation of uniform unilamellar nanovesicles using CO_2-expanded solvents

M. Cano, S. Sala, N. Ventosa and J. Veciana**

Dept. Nanociencia Molecular y Materiales Orgánicos
Institut de Ciències de Materials de Barcelona (CSIC)-CIBER-BBN,
Campus de la UAB 08193 – Barcelona, Spain
Contact e-mail: **ventosa@icmab.es; **vecianaj@icmab.es***

Advances in the preparation of materials characterised by exceptional properties attributable to their nanoscopic structure, such as nanosuspensions, nanospheres, nanoparticulate composites, etc. are crucial to the development of important industrial sectors, such as drug manufacturing. Herein we present a novel easy to scale-up precipitation procedure, based on the use of compressed fluids, for the robust preparation in a single-step, of nanoscopic sized, stable, uniform shaped and unilamellar lipid vesicles in an aqueous phase, unachievable by conventional procedures, with potential applications in drug- and contrast agent- delivery.

Keywords: vesicles, compressed fluids, carbon dioxide, drug-delivery

Introduction

From an aesthetic perspective, it is attractive to build all desirable pharmacological features of a drug such as solubility, stability, permeability to biological membranes, and targeting to particular tissues, cells, and intracellular compartments into the drug molecule itself. But it is simpler and perhaps more powerful obtaining these features by decoupling the biological action of the drug from the other biochemical and physicochemical characteristics that determine these key features of its pharmacology. **[1]** In accordance with this strategy, the obtaining of new micro- and nanostructured molecular materials and the understanding of how to manipulate them at nanoscopic level, are currently playing a crucial role in drug delivery and clinical diagnostics. It has been observed that polymer nanoparticles, **[2-6]** micelles, **[7]** nanoemulsions, nanosuspensions, **[8]** vesicles, **[9,10]** are efficient devices, which can significantly help to develop new drug delivery routes, more selective and efficient disease-detection systems, drugs with a higher permeability to biological membranes with controlled released profiles, and to enhance their targeting towards particular tissues, cells or intracellular compartments.

Vesicles are sub-microscopic (<500nm) sacs that enclose a volume with a molecularly thin membrane. The membranes are generally self-directed assemblies of amphiphilic molecules with a dual hydrophilic-hydrophobic character (see **Figure 1**). In nature, large lipid vesicles function as membranes in biological cells to protect the intracellular components from the extracellular environment, and small lipid vesicles (nanometers in size) function to transport biomolecules intracellulary. Vesicles are particularly attractive for drug delivery, since they may permit to incorporate larger molecules than micelles, independent of the molecule identity. Such systems may also provide unprecedented protection of the drug from biological degradation and denaturation before entry into the cell **[9].**

In this context, uniform and small unilamellar vesicle (SUV) systems are attracting a great deal of interest as intelligent materials for drug-delivery since they can be used as containers sensitive to external stimuli-pressure, pH, temperature or concentration changes in the medium-triggering modifications in their supramolecular structures (see **Figure 2**) **[11].** Drugs can interact with vesicles in several different ways depending on their solubility and polarity characteristics. Indeed, they can be inserted in the lipid chain bilayer region, intercalated in the polar head group region, adsorbed on the membrane surface, anchored by a hydrophilic tail or entrapped in the inner aqueous vesicle core.

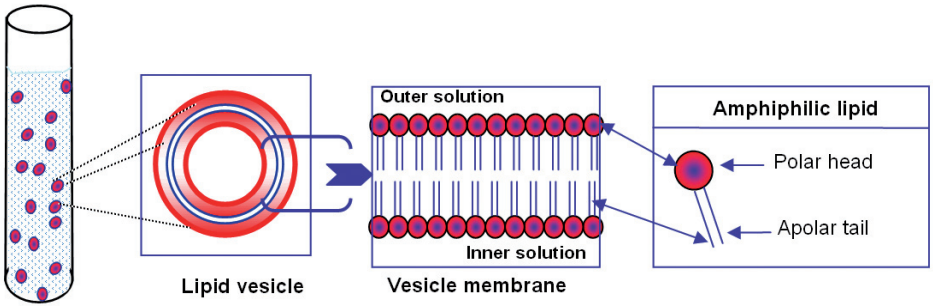

Figure 1. *Schematic drawing of the self-assembling of amphiphilic molecules into vesicles when they are dispersed into an aqueous environment.*

The control of the nanostructure - particle size distribution, membrane morphology and supramolecular organization - of these vesicular systems is of profound importance for their applications in material science and for drug delivery purposes. Important pharmacological features of lipid

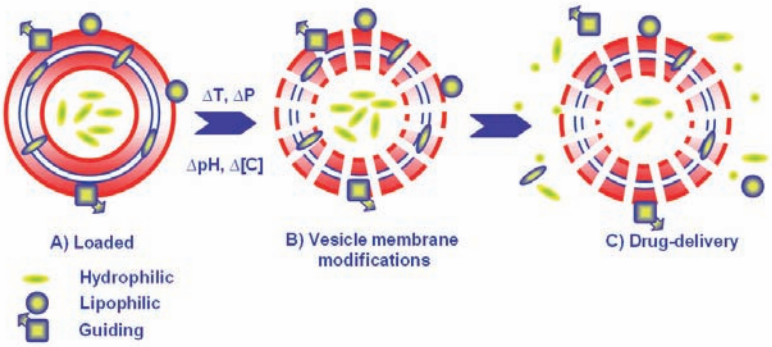

Figure 2. *Nanovesicle for drug delivery: **A)** Loaded vesicle with lipophilic or/and hydrophilic drugs and guiding molecular units. **B)** Temperature, pressure, concentration or pH changes in the external medium can modify the membrane supramolecular organization and its permeability. **C)** Encapsulated drugs in the vesicle, either in the aqueous internal medium or linked at the membrane are delivered through the membrane into tissues, cells or intracellular compartments.*

vesicles, such as stability, loading capability, leakage kinetics of the entrapped substances, and response speed to external stimuli are tightly related to its nanostructure **[11].** Therefore, the development of reproducible, efficient, environmental friendly and easy to scale-up methodologies for the production of vesicular systems with controlled sizes and supramolecular organizations is of great industrial interest **[12,13].**

Although, a vast of techniques have been developed for lipid vesicle synthesis, there still exist many drawbacks. For example, lipid vesicle systems in aqueous phases are currently prepared by conventional mixing technologies producing multilamellar vesicles (MLVs) which must be sonicated and extruded down through filters of a defined pore size until uniform unilamellar vesicles are obtained **[14].** Such mixing methods have several problems associated that can be summarized as follows: multiple steps of preparation, low reproducibility, long processing times, high consumption of energy, and limited control of particle sizes over the final particulate material. These disadvantages are mainly originated because these solvent-based processes are driven by composition changes on the processed systems, which are slowly and non-homogeneously transmitted in liquid media **[15].** In these technologies, high stirring efficiencies are required in order to minimize the obtaining of undesired MLVs, and consequently the scale-up of these vesicle preparation procedures is always problematic. More recently, a novel method for lipid vesicle preparation has been developed using a droplet based microfluidic system **[16].** This single-step process enables a high control and government of the final vesicle structural characteristics. But again, its scale-up is not easy since high technological inputs and complex equipments are required.

In contrast with liquid solvents, the solvent power of compressed fluids (CFs), either in the liquid or supercritical state, can be tuned by pressure changes, which propagate much more quickly than temperature and composition solvent changes. Therefore, processes using CFs allow a much greater control and tuning of the structural characteristics of the final material (size, size distribution, porosity, polymorphic nature, morphology, etc.) than with conventional organic liquid solvents. Indeed, processing with CFs often leads to materials with unique physicochemical characteristics, unattainable by conventional processing methodologies in liquid solution. The most widely used CF is compressed CO_2 (cCO_2), which is non-toxic, non-flammable, cheap and easy recyclable. It has gained considerable attention, during the past few years as a «green substitute» to organic solvents and even water in industrial processing. During the past two decades, «bottom-up» approaches using cCO_2 as a solvent medium have attracted scientific and technological interest for the preparation of nanostructured materials, such as particles, fibres, templates, porous materials, etc. **[17-23].**

Vesicle preparation using CO_2-expanded solvents

Herein we present a novel method **[24]** which uses compressed CF for the straightforward preparation of uniform unilamellar nanovesicles systems. As schematized in **Figure 3**, the lipidic substance is first dissolved in a conventional organic solvent, at atmospheric pressure and at a working temperature, T_W. A CF (eg. CO_2) is added in order to obtain a volumetric expanded solution of the lipid, at the temperature T_W and at high pressure (P_W), with a given molar fraction of CO_2, X_W. This CO_2-expanded solution is depressurized, from P_W to atmospheric pressure, over a continuous aqueous flow to give uniform unilamellar lipid nanovesicles. In some cases, the aqueous flow could contain surface-active compounds. During the depressurization stage, the solution experiences a large, fast and extremely homogeneous temperature decrease, caused by the evaporation of the CO_2 from the expanded solution **[25].** This extremely uniform temperature decrease over all the solution, provokes the nucleation of the lipid molecules, with the same extent at any point of the solution. This may explain the small size and morphological uniformity of the final vesicles achieved when the depressurized solution is mixed with the aqueous flow. We have used this novel method for preparing in a single step, nanosized, stable, uniformly shaped, and unilamellar rich in unilamellar-rich coles-5-en-3β-ol (cholesterol) vesicles, unachievable by conventional procedures. The cholesterol is a functional lipid practically insoluble in water and somewhat soluble in supercritical CO_2, which is amply used as an active substance in cosmetic, nutraceutical, and pharmaceutical products **[26].** The majority of vesicular systems are based on phospholipids (liposomes); however, there has been a continuous interest in preparing vesicules from non-phospholipid amphiphiles, such as cholesterol **[27].** This kind of vesicular formulation shows a lower passive leakage than liposomal systems, and therefore, they have a higher ability to encapsulate materials, for example, therapeutically active molecules. For the preparation of the rich cholesterol nanovesicles, we have used acetone organic solvent, and a 1% of surfactant cetyltrimethylammonium bromide (CTAB) was present in the aqueous flow **[24].** The particle size characteristics of the vesicular system prepared were measured by dynamic light scattering (DLS), and the stability was stu-

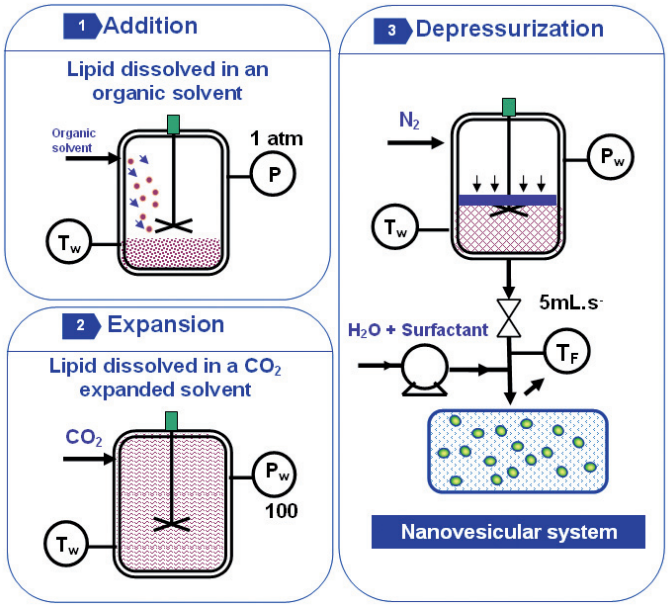

Figure 3. *Schematic three main steps for the preparation of nanovesicles using CO_2-expanded solvents.*

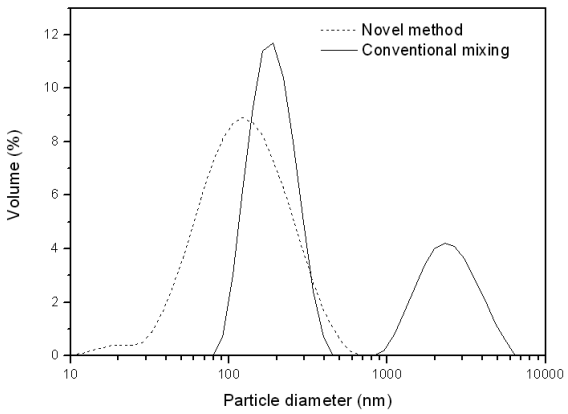

Figure 4. *Particle size distribution curves measured by dynamic light scattering of rich cholesterol vesicles prepared by the novel method from CO_2-expanded acetone (dashed line) and by conventional mixing method (continuous line). Curves are represented in terms of particle volume percentage* ***[24].***

died by measuring the ζ potential and the turbidity of the dispersed system through its backscattering and transmission profiles. Worth mentioning are the differences in the physicochemical characteristics of cholesterol vesicular systems obtained by the novel method, from CO_2-expanded acetone, and by a conventional mixing method operating at the same process conditions, but without performing the expansion with CO_2 of the solution of cholesterol in acetone. Thus, the vesicles produced by the new procedure have a mean particle size (167nm) smaller than the ones formed through the conventional mixing method (301nm), as well as a remarkable unimodal and narrow particle size distribution (**Figure 4**). Moreover, the vesicles formed using cCO_2 were more stable than the conventional mixing ones, as the novel method produced vesicles have a ζ potential more positive (+88.8mV) and a migration velocity 5 times lower (0.22m/s) than those prepared through the conventional mixing method (+31.3mV, 1.17μm/s).

The morphology of the samples was examined using cryogenic transmission electron microscopy (cryo-TEM). As it is observed in **Figure 5 page 31, right image**, the vesicular system produced by the new cCO_2 based method, is constituted by extremely uniform spherically shaped vesicles, which in all cases are unilamellar. The observed vesicles have a mean size centred on 200nm, in good agreement with DLS measurements. In contrast, with the conventional mixing method, a multilamellar vesicular system, formed by multiple and concentric bilayers with a bigger and less homogeneous particle size distribution, is obtained (**left image, Figure 5 page 31**).

As shown in Figure 5, the properties of the vesicular system prepared by the CO_2-based method do not change noticeably over periods of several months while the dispersed systems obtained with the mixing methodology are unstable in a few weeks. Indeed, DLS measurements showed that vesicles prepared by the novel method have much higher mean particle size stability as a function of time than those obtained by conventional mixing. Thus, the as-prepared sample shows a mean size of 167nm which remains constant after 6 months (171nm) while the

Advertisement

Figure 5. Cryo-TEM micrograph images of cholesterol vesicular systems prepared by the novel method using cCO_2 (image A) and by conventional mixing (image B). Central photograph: rich in cholesterol vesicular systems after one month of being prepared by the conventional mixing method (left two samples) and by the cCO_2 based novel method (right sample).

as-prepared sample, by conventional mixing, shows a mean size of 301nm which increases considerably after 6 months (26μm).

Conclusion

We conclude that stable and structurally well-defined uniform spherically shaped, unilamellar rich cholesterol nanovesicles dispersed in an aqueous phase are formed by a novel cCO_2 process showing physicochemical characteristics unachievable by conventional mixing technologies. It is worth mentioning that this process overcomes some of the limitations related to traditional methods for preparing nanovesicles, offering alternative advantages for clean and nontoxic drug formulations and clinical diagnosis. For instance, design of the stirring system, which is usually a problem in many conventional mixing industrial processes for vesicles preparation, is not a key point. Moreover, it can be scaled up easily, producing large amounts of the dispersed vesicles. Application of this new technology for encapsulating bioactive compounds, inside the water-dispersed nanovesicles, in order to improve its delivery is currently in progress.

References

[1] Hubell, **J.A. Science 2003, 300, 595.**
[2] Bader, H.; Ringsdorf, H.; Schmidt, B; **Angew. Makromol. Chem. 1984, 123-124, 457.**
[3] Dreher, M. R.; et al. **J. Natl Cancer Inst. 2006, 98, 335.**
[4] Duncan, R.; **Nature Rev. Drug. Discov. 2003, 2, 347.**
[5] Shiah, J. J.; Sun, Y.; Peterson, C. M.; Kopecek, J.; **J. Control Release 1999, 61, 145.**
[6] R.H. Müller, K. Mäder, S. Gohla, **"Solid lípid nanopartícles for controlled drug delivery- a review of the state of the art" 2000, 50, 161**.
[7] Savic, R.; Luo, L.; Eisenberg, A.; Maysinger, D.; **Science 2003, 300, 615**
[8] Rabinow, B.E.; **Nature Reviews, 2004, 3, 785.**
[9] Discher, D.E.; Eisenberg, A.; **Science 2002 297, 967.**
[10] Wright, S.; Huang, L. **Adv. Drug Delivery Rev. 1989, 3, 343.**
[11] (a) Hafez, I.M.; Cullis, P.R. **Advanced Drug Delivery Reviews 2001, 47, 139**; (b) Gabrielle-Madelmont, C.; Lesieur, S.; Ollivon, M. **J. Biophys. Methods 2003, 56, 189.**
[12] Torchilin, **P. Nature Reviews, 2005, 4, 145**
[13] H. Möhwald, **Soft Matter, 2005, 1, 328.**
[14] (a) Lesieur,S. ; Gabrielle-Madelmont, C. ; Paternostre, M-T. ; Moreau, J-M. ; Handjani-Vila, R-M. ; Ollivon, M. **Chemistry and Physics of Lipids 1990, 56, 109** (b) Bastiat, G. ; Olinger, P. ; Karlsson,G. ; Edwards,K. ; Lafleur, M. **Langmuir 2007, 23, 7695**
[15] (b) Müller, R.H.; Benita, S.; Böhm, B. **Emulsions and nanosuspensions for the formulation of pooly soluble durgs, Medpharm Publishers, Stuttgart 1998.** (c) Müller, R.H.; Mäder, K.; Gohla, S.; **Eur. J. Pharm. and Biopharm. 2000, 164, 50, 161.**
[16] Tan Y-Ch.; Hettiarachchi, K.; Siu M.; Pan Y-R.; Lee A.P., **J. Am. Chem. Soc. 2006, 128, 5656**.
[17] Y.-P. Sun (Ed.), **Supercritical Fluid Technology in Material Science and Engineering, Marcel-Dekker, New York, 2002**
[18] P. G. Jessop, W. Leitner (Eds.), **Chemical Synthesis Using Supercritical Fluids, Wiley-VCH, Weinheim, 1999**.
[19] (a) Pathak, P.; Meziani, M.J.; Desai, T.; Sun,Y-P. **J. Am. Chem. Soc. 2004, 126, 10842.** (b) Meziani, M.J.; Sun, Y.-P. **J. Am. Chem. Soc. 2003, 125, 8015**.
[20] Munto, M.; Gomez-Segura, J.; Campo, J.; Nakano, M.; Ventosa, V.; Ruiz-Molina, D.; Veciana, **J. J. Mater. Chem. 2006, 16, 2612**.
[21] (a) Ventosa, N.; Sala, S.; Torres, J.; Llibre, J.; Veciana, **J. Cryst. Growth. Des. 2001, 1, 299.** (b) Gimeno, M.; Ventosa, N.; Sala, S.; Veciana, **J. Cryst. Growth. Des. 2006, 6, 23.** (c) Ventosa, N.; Veciana, J.; Rovira, C.; Sala, S. **(Carburos Metálicos S.E), Patent WO0216003**
[22] J. D. Holmes, Lyons D.M.; , Ziegler, K.J.; **Chem. Eur. J., 2003, 9, 2144**.
[23] Ventosa, N.; Veciana, J.; Sala, S.; Muntó, M.; Cano, M.; Gimeno, M. **Contribution to Science 2005, 3, 11**.
[24] Cano-Sarabia M., Ventosa, N., Sala, S., Patiño C., Arranz R., Veciana, J., **Langmuir, 2008, 24, 2433**.
[25] Ventosa, N.; Sala, S.; Veciana, **J. J. Supercritical Fluids 2003, 26, 33**
[26] (a) Tan, C.P; Nakajima, M. **Food Chemistry 2005, 92, 661.** (b) Türk, M.; Lietzow, R. **Biotechnol. Prog. 2000, 16, 402**.
[27] Philippot, J.R.; Milhaud, P.G.; Puyal, C.O.; D.F.H. **Wallach In Liposomes as Tools in Basic Research and Industry;** J. R. Philippot, F. Schuber, **Eds.; CRC Press: Boca Raton, FL 1995; pp 41-75**.

Optical Resonances in Finite Arrays of Dielectric Nanorods

S. Albaladejo[(1)], M. Laroche[(2)] and J.J. Sáenz[(1)]

[(1)]Moving Light and Electrons (MOLE) Group, Departamento de Física de la Materia Condensada, Universidad Autónoma de Madrid, 28049-Madrid, Spain.
[(2)]Laboratoire EM2C, CNRS, Ecole Centrale Paris, 92295 Châtenay-Malabry, France

1. Introduction.

Understanding absorption and extinction processes in nanoparticle arrays **[1]** is a key issue in nanoscience and technology and has considerable interest for their potential applications to chemical and biological sensors as well as for surface enhanced Raman scattering (SERS) **[2]**. Tailoring the absorption and thermal emission is especially relevant for thermophotovoltaic (TPV) applications and for the design of efficient light and infrared sources. For instance, photonic crystals and nanoparticle arrays can be used as efficient selective emitters **[3]**. The interesting properties of these systems are usually attributed to the excitation of localized surface states **[4]**, plasmon/phonon-polariton **[1,5]** resonances or guided modes **[6]** that are subsequently diffracted by the micro/nanostructured lattice periodicity. Simple subwavelenght cylinder arrays have been shown to present striking emission/absorption and extinction resonances **[7-9]**. In this case the periodic

structure itself leads to both localized and diffracted modes which give rise to geometric "lattice" resonances **[7,10].**

Most of previous theoretical works lead to infinite periodic structures illuminated by plane waves. In this work we discuss the optical resonances in finite arrays of dielectric nanorods. We will show that a finite system illuminated by a focused beam present resonant properties that strongly resembles those predicted for infinite periodic nanoparticle arrays. We will see that it is possible to tune the resonant properties of finite arrays of dielectric nanorods for different specific purposes relevant for TPV, SERS and fluorescence enhancement biosensors.

2. Scattering from a finite system of dielectric nanorods

The scattering properties of a finite system of dielectric nanorods can be calculated by using a couple dipole method (CPM) **[11]**. For simplicity we shall focus on the scattering of TM or *s* polarized electromagnetic waves (with the incoming electric field along the cylinder axis). Here we will follow the approach introduced by Albaladejo et al. **[12]** to analyze the properties of waveguides built into finite photonic crystals. We consider a finite set of parallel cylinders with their axis along the z axis, relative dielectric constant $\varepsilon=\varepsilon'+i\varepsilon''$ and radius a much smaller than the wavelength. The system, together with the definition of some relevant parameters is sketched in **Figure 1**. A Gaussian beam, $E_{inc}(x,y)$ $\mathbf{u}_z$ of width W_0, focused on the surface (x=y=0), is incident upon the system from y<0 with

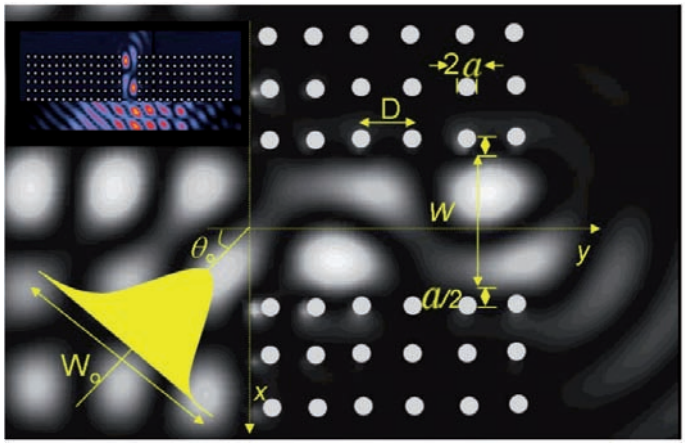

***Figure 1**. Sketch of a finite system of nanorods including the definition of relevant parameters. Inset: scheme of the structure of a photonic crystal waveguide of variable width illuminated by a Gaussian beam. The intensity map corresponds to actual calculations of the electric field intensity (with the electric field perpendicular to the plane of the figure). Calculations correspond to Si nanorods in air with D=0.6μm, a/D=0.16, λ=1.33μm, and θ_0=45°. In this particular case W=2D **[After Ref. 12]**.*

wave vector $\mathbf{k}_0 \perp \mathbf{u}_z$ ($\mathbf{k}_0=k\sin\theta\mathbf{u}_x+k\cos\theta\mathbf{u}_y$ and k=w/c). The field scattered from a single subwavelenght cylinder n for cylindrical waves can be written as

$$E_n^{scatt}(\vec{r}) = \alpha_{zz} E_{in}(\vec{r}_n) k^2 G_0(\vec{r},\vec{r}_n) \qquad (1)$$

where

$$G_0(\vec{r},\vec{r}_n) = \frac{i}{4} H_0(k|\vec{r}-\vec{r}_n|)$$

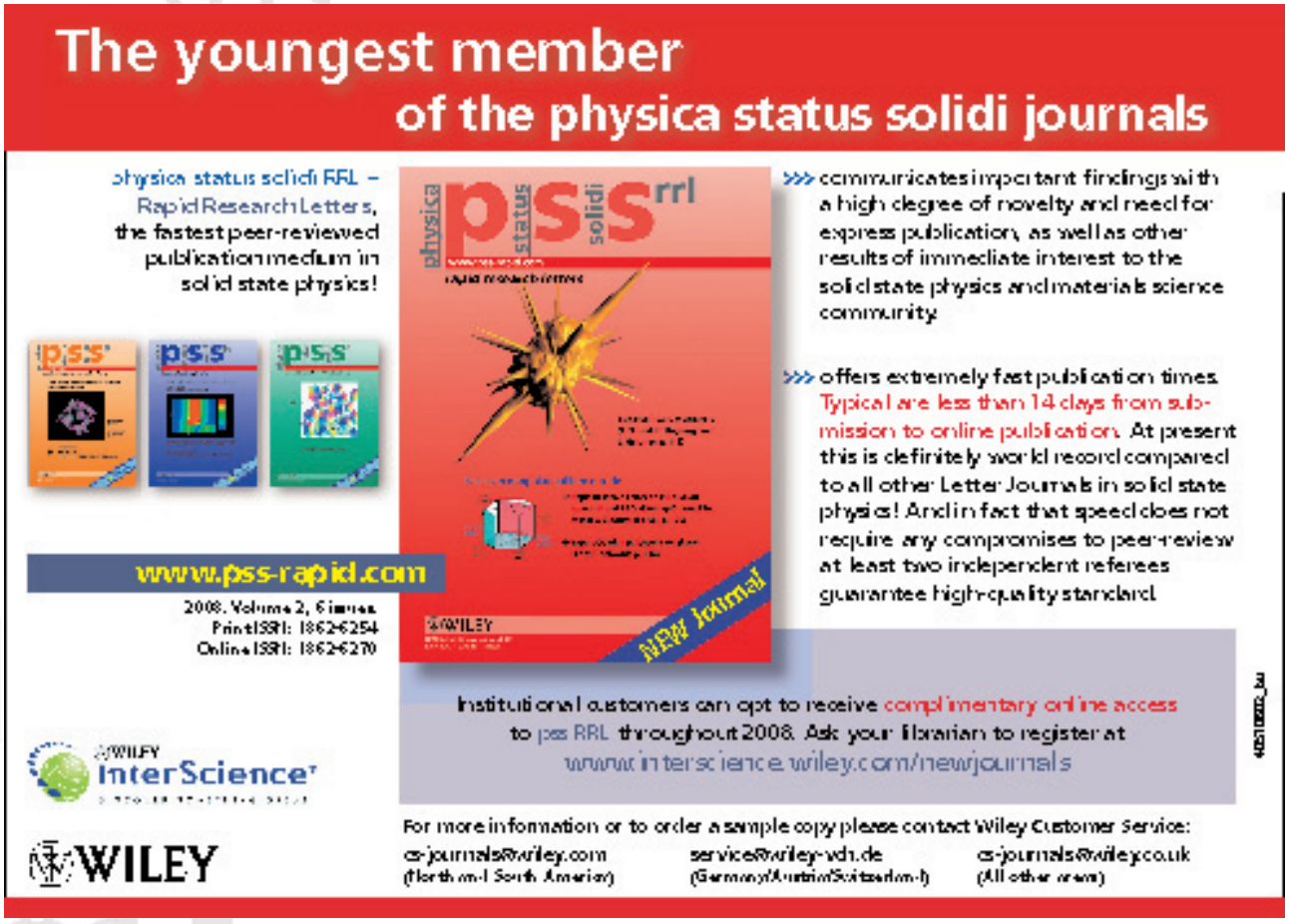

is the free-space Green function,

$E_{in}(\vec{r}_n)$

is the incident field on the scatter and, in the small particle limit, the polarizability $\alpha_{zz}$is given by **[12]**

$$\alpha_{zz} = \pi a^2 (\varepsilon - 1)\left[1 - i\frac{\pi}{4}(ka)^2(\varepsilon - 1)\right]^{-1} \quad (2)$$

The total incoming field on a given cylinder

$E_{in}(\vec{r}_n)$

is obtained self-consistently from the solution of

$$(\vec{r}_n) + \sum_{j \neq n} k^2 G_0(\vec{r}_n, \vec{r}_j)\alpha_{zz} E_{in}(\vec{r}_j) \quad (3)$$

3. Absortion and extinction in nanorod arrays

Let us now consider the simple case of a one-dimensional array of nanorods. The dielectric rods are located at $\mathbf{r}_n = nD\mathbf{u}_x = x_n\mathbf{u}_x$ (with n an integer number). For an infinite periodic system, the reflectance R and the transmittance T of the cylinder array can be calculated by using a multiple scattering approach in the dipolar approximation **[7-9]**. The absorptivity, A, defined as A ≡1-R-T and the normalized extinction E (the ratio between scattered plus absorbed powers and incoming power) can be expressed in terms of α_{zz},

$$A^{(s)} = \frac{C\varepsilon''}{Dk_y}\left[\mathrm{Re}^2\left[\frac{1}{k^2\alpha_{zz}} - G_b\right] + \left[C\varepsilon'' + \mathrm{Im}\{G\}\right]\right] \quad (4)$$

$$E^{(s)} = A^{(s)} + \frac{k^4|\hat{\alpha}_{zz}|^2}{Dk_y}\left(\mathrm{Im}\{G\} - \frac{1}{4Dk_y}\right) \quad (5)$$

where G_b is the depolarization term and G is the Green function of the periodic array **[8]**.

Resonant absorption/extinction takes place when

$$\mathrm{Re}\left(\frac{1}{(k^2\alpha_{zz})} - G_b\right) = 0 \quad (6)$$

Approaching the threshold of the first diffracting channel, the real part of G_b goes to infinity as $\approx (\omega^2_1 - \omega^2)^{-1/2}$ c/(2D) and can compensate exactly the real part of $1/k^2\alpha_{zz}$ giving rise to a ''geometric lattice'' resonance **[7-10]**. This can only happen when the real part of the polarizability is positive. As a consequence, for metallic cylinders in "*s*" polarization there is no resonant absorption.

Figure 2 illustrates a typical extinction spectra for SiC nanowires with a dielectric constant given by $\varepsilon = \varepsilon_\infty(\omega^2_L - \omega^2 - i\gamma\omega)/\omega^2_T - \omega^2 - i\gamma\omega$ (with the following parameters **[13]**: $\varepsilon_\infty = 6.7$, $\omega_L = 1.8251014$ rad s^{-1}, $\omega_T = 1.4941014$ rad s^{-1}, $Y = 8.96621011$ rad s^{-1}). It is worth noticing that exactly at Rayleight frequency, $\omega = \omega_1$, the array of cylinders is transparent as the absorption/extinction goes to zero. While it is possible to obtain a 100% extinction of the beam, the maximum absorption A_{max} is limited to 50% for "*s*" polarization. It can be shown **[8]** that the highest absorption, $A_{max}=1/2$ takes place below the Rayleigh frequency when

$$C\varepsilon'' = \frac{Q_0^2}{k^2}\frac{1}{2Dk_y} \quad (7)$$

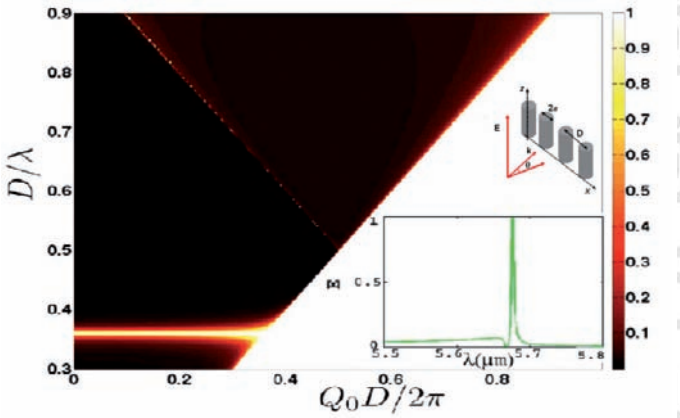

Figure 2. *Extinction in s-polarization in a map of frequency vs. the transversal momentum of incoming radiation for an infinite array of SiC nanocylinders with period D=4.5μm and radius a=0.2μm. The inset shows the extinction spectrum, which exhibits a typical fano line shape, for an incident angle θ=15º around the geometric resonance* ***[After Ref. 8]***

In order to tackle more realistic problems it is important to know the behaviour of finite systems. Even for a relatively small number of cylinders, the results for a finite system are similar to those obtained for an infinite periodic array. This is shown in **Figure 3**, where we compare the reflection coefficient versus wavelength of an infinite array with a system of 20 nanorods. For the finite system, the reflectance does not go to zero at the Rayleigh frequency due to an effective average over angles of incidence associated to the finite width of the Gaussian beam. However, the sharp peak in the reflectance remains even for a very small number of nanorods

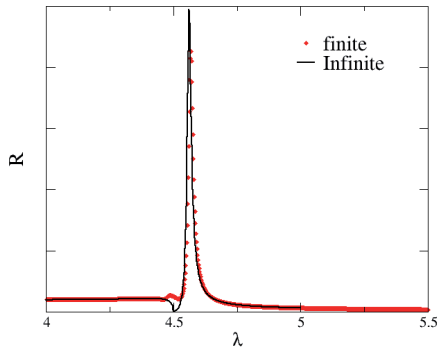

Figure 3. *Reflectance coefficient for a finite (20 rods) and infinite array of SiC nanorods with D=4.5μm and a=0.2μm and normal incidence (the beam width is 15μm).*

4. Field enhancement resonances in nanorod arrays

A one-dimensional array of dielectric nanorods can produce substantial local field enhancement FE. In the search for devices producing an enhancement of molecular fluorescence, the most common approach is the use of metallic nanostructures, which are expected to produce strong local field enhancements (FEs). A drawback when using metals is the presence of absorption, which creates additional nonradiative decay channels. In contrast, FE in non-absorbing dielectric structures would directly translate into the enhancement of the fluorescence signal without quenching **[9]**.

To illustrate this resonant enhancement, we consider a system of $Ti0_2$ nanorods with a dielectric constant ε=6.1,

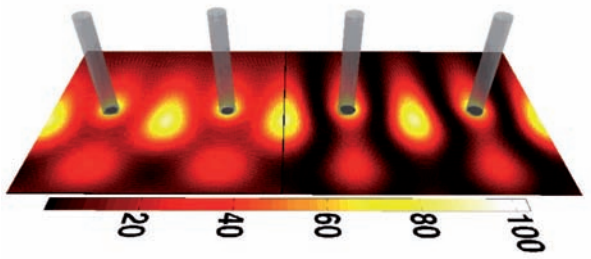

Figure 4. Normalized total field intensity (FE) map at resonance in an array of TiO_2 nanorods with radius α=40nm (λ=800nm, d=783.6nm, and normal incidence θ=0º).The half map on the left correspond to a finite array of 30 nanorods and the right one to an infinite array.

for wavelengths $\lambda \approx 0.8\mu m$. **Figure 4** illustrate the spatial distribution of the field enhancement in resonant conditions. This field amplification takes place exactly at the wavelength of the geometric reflection resonances. Just at resonance, the field enhancement is very large not only on the rod surface but also in the centre between rods in both finite and infinite system **[9,14]** (see Figure 4).

As shown in **Figure 5**, field enhancement factors up to 100 are possible for "*s*" polarization and realistic values of the parameters. At normal incidence the resonant condition occurs at periods slightly smaller than the wavelength ($d \leq 0.8\mu m$) as shown in the inset of Figure 3. Similar values can also be found for finite nanorod arrays **[14]**. A careful alignment between the light beam and the array could then lead to huge FE with intriguing applications.

Conclusion

We have discussed the optical properties of finite arrays of dielectric nanorods. The existence of geometrical absorption resonances, even for finite systems, is especially relevant for TPV applications. We have shown that a finite array of transparent dielectric nanorods could produce substantial local FE, which could directly translate into the enhancement of the fluorescence signal without quenching. Our results should also have important applications in surface-enhanced Raman scattering **[2]** or surface-enhanced infrared absorption **[15]**, where controlling the local field enhancement is a key issue.

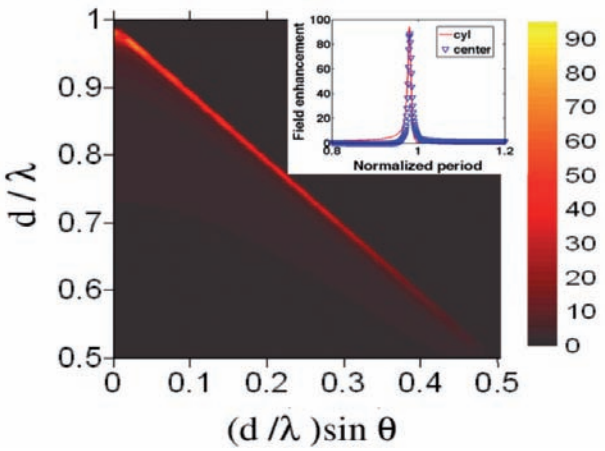

*Figure 5. Field enhancement factor in a period d/λ versus in-plane wavenumber (d/λ) sinθ map calculated at fixed λ=800nm for an array of TiO_2 nanorods. Inset: FE versus the period at normal incidence (both on the surface and in the center between rods) **[After Ref. 9].***

Acknowledgements

The authors thank R. Carminati, L.S. Froufe-Pérez and R. Gómez-Medina for interesting discussions. This work has been supported by the Spanish MEC (Ref. No. FIS2005-05137, FIS2006-11170-C02-02 and NanoLight Consolider -CSD2007-00046-), Microseres-CM and the EU-IP "Molecular Imaging" (LSHG-CT-2003-503259).

References

[1] B. Lamprecht et al. **Phys. Rev. Lett. 84, 4721 (2000)**; N. Félidj et al., **Phys. Rev. B 66, 245407 (2002)**; Q.-H. Wei, K.-H. Su, S. Durant, and X. Zhang, **Nano Lett. 4,1067 (2004)**; E. M. Hicks et al., **Nano Lett. 5, 1065 (2005).**

[2] K. Kneipp et al., **Phys. Rev. Lett.78, 1667 (1997)**; S. Nie and S. R. Emory, **Science 275, 1102 (1997)**. S. J. Oldenburg et al., **Chem. Phys. Lett. 288, 243 (1998)**. A. N. Shipway, E. Katz, and I. Willner, **ChemPhysChem 1, 18(2000)**; L. Qin et al., **Proc. Natl. Acad. Sci. U.S.A. 103, 13300 (2006).**

[3] S. Y. Lin et al., **Phys. Rev. B 62, R2243 (2000)**; S. Enoch et al., **Appl. Phys. Lett. 86, 261101 (2005)**.

[4] M. Laroche, R. Carminati, and J.-J. Greffet, **Phys. Rev. Lett. 96, 123903 (2006).**

[5] J.-J. Greffet et al., **Nature (London) 416, 61 (2002).**

[6] H. Rigneault et al., **Opt. Lett. 24, 148 (1999)**; A.L. Fehrembach and A. Sentenac, **Appl. Phys. Lett. 86, 121105 (2005).**

[7] R. Gómez-Medina, M. Laroche, and J. J. Sáenz, **Opt. Express 14, 3730 (2006).**

[8] M. Laroche, S. Albaladejo, R. Gómez, and J.J. Sáenz, **Phys. Rev. B 74, 245422 (2006).**

[9] M. Laroche, S. Albaladejo, R. Carminati and J.J. Sáenz, **Opt. Lett. 32, 2762 (2007).**

[10] F. J. García de Abajo, R. Gómez-Medina, and J. J. Sáenz, **Phys. Rev. E 72, 016608 (2005)**; F. J. García de Abajo, and J. J. Sáenz, **Phys. Rev. Lett. 95, 233901 (2005).**

[11] B. T. Draine, **Astrophys. J. 333, 848 (1988)**; D. Felbacq, G. Tayeb, and D. Maystre, **J. Opt. Soc. Am. A 11, 2526 (1994)**; E. Centeno and D. Felbacq, **Opt. Commun. 160, 57 (1999)**.

[12] S. Albaladejo et al., **Appl. Phys. Lett. 91, 061107 (2007).**

[13] E. D. Palik, **Handbook of Optical Constants of Solids Academic, San Diego, (1985)**.

[14] S. Albaladejo et al., **to be published (2008)**.

[15] R. F. Aroca, D. J. Ross, and C. Domingo, **Appl. Spectrosc. 58, 324A (2004).**

nanotimes

Experience the virtual SPM

" How can I speed up my SPM research ? "

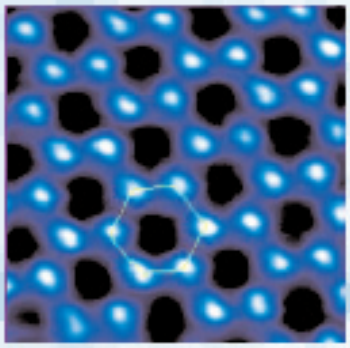

Experimental image

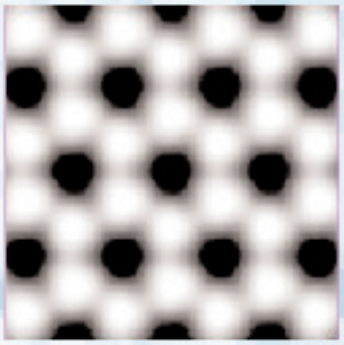

Simulated image

The SPM simulation software provider

Try our products for free now !

Nt_STM
Nt_AFM
Nt_SCHOLAR

www.nanotimes.fr

Tel: +33 9 52 45 51 77

SURFACE ANALYSIS

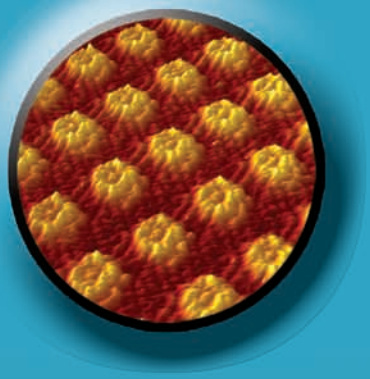

AFM / STM

Materials, polymers, biology, electrochemistry...

SNOM Microscopy

Reflection, transmission, Apertureless...
SECM, Deep Trench, nanopipette probes...

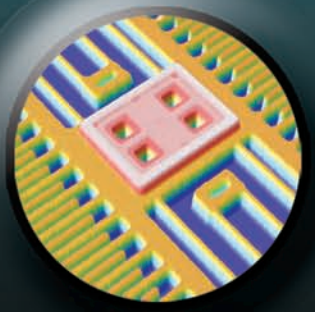

3D Optical Profilometry

New confocal technology...
Interferometry (PSI/VSI)...

And also...

Mechanical profilometry, nano-indentation...

ScienTec FRANCE
17 Av. des Andes - Batiment le Cèdre
91940 LES ULIS
Tel : + 33 (0)1 64 53 27 00

ScienTec IBERICA
C/Buenavista 4, Bajos
28250 Madrid - ESPAÑA
Tel : + 34 918 429 467

www.scientec.fr / info@scientec.fr